HPXM2023 - High Precision X-ray Measurements
19-23 June 2023 – INFN-LNF

Comparison of characteristics and performance between the new detection system based on Silicon Drift Detectors of XAFS beamline of Elettra and SESAME

Daniela Cirrincione
INFN-Trieste

RESEARCH
DRIFT
FOR
SOFT
X-RAYS

Abstract

The collaboration between INFN-Trieste, TIFPA, FBK, the Politecnico di Milano and Elettra-Sincrotrone Trieste over the past few years has led to the design, production and deployment of two state-of-the-art instruments that now equip the XRF/XAFS beamline of the SESAME synchrotron and the XAFS beamline of Elettra.
Both these instruments are 64-channels modular detection systems based on monolithic array of Silicon Drift Detectors (SDD). Detection systems have large total collection area, capable of operating with low dead time and high count rate. They present excellent performance already at room temperature: an energy resolution at the Mn 5.9 keV Ka line below 170 eV FWHM. These instruments are similar but have their own unique and different characteristics due to the construction experience and the particular requirements of the beamline scientists who collaborated in the development of the detector systems, such as the new collimation system installed on the Elettra's instrument. In addition, they are optimised and seamlessly integrated with the beamlines for which they were designed.

D. Cirrincione*a,b, G. Agostini c, M. Antonelli a, G. Aquilanti c, P. Bellutti d,e, G. Bertuccio f, G. Borghi d,e, G. Cautero c,a, F. Ficorella d,e, M. Gandola f, D. Giuressi c,a, F. Mele f, R. H. Menk c,a, L. Olivi c,a, G. Orzan a, G. Pepponi d,e, A. Picciotto d,e, I. Rashevskaya e, A. Rachevski a, L. Stebel c, G. Zampa a, N. Zampa a,b, N. Zorzi d,e, A. Vacchi b,a

a INFN Trieste, Padriciano 99, Trieste, I-34149, Italy,
b DMIF, University of Udine, Via delle Scienze 206, Udine, I-33100, Italy,
c Elettra-Sincrotrone Trieste, s.s. 14 km 163,500 in Area Science Park, Trieste, I-34149, Italy,
d Fondazione Bruno Kessler, Via Sommarive 18, Trento, I-38123, Italy,
e TIFPA – INFN, Via Sommarive 14, Trento, I-38123, Italy,
f Politecnico di Milano, Via Anzani 42, Como, I-22100, Italy,

RESEARCH DRIFT FOR SOFT X-RAYS redSox

INFN Istituto Nazionale di Fisica Nucleare · TIFPA · INAF Istituto Nazionale di Astrofisica · FONDAZIONE BRUNO KESSLER · Elettra Sincrotrone Trieste · Politecnico Milano · Universitas Studiorum Utinensis

- Development of high energy resolution SDD for soft X-rays
- Evolution of SDD technology in collaboration with FBK CMM Trento
- Evolution of FE electronics in collaboration with PoliMI
- Development of large surface SDD for X-ray astrophysics
- Development of detection systems for Advanced Light Sources

Scientific and technological applications of SDD

- X-ray Astrophysics
- Gamma-ray Astrophysics
- Advanced Light Sources
- Biophysics
- Medicine
- Nanotechnology
- Materials science
- Industry
- Cultural heritage

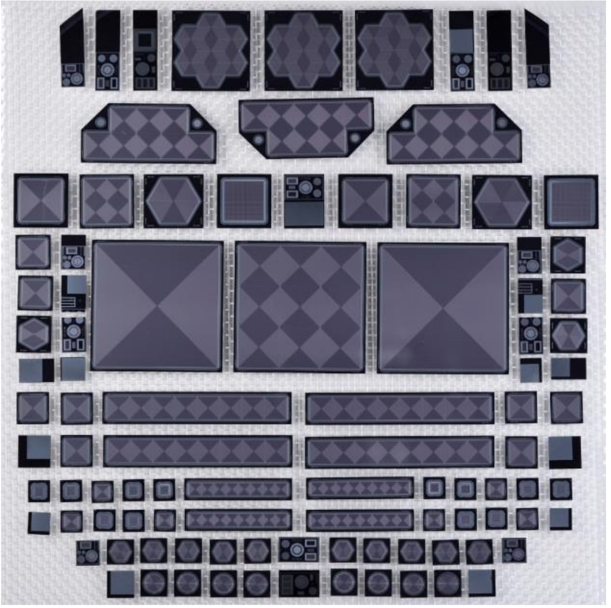

Ongoing developments: from prototypes to detectors

Improvement and detailed study to have:

- Detector optimization
- Excellent energy resolution performances at room temperatures
- Dedicated design of sensors and electronics for each application
- Reliability
- Repeatability

X-Ray Fluorescence (XRF) spectroscopy

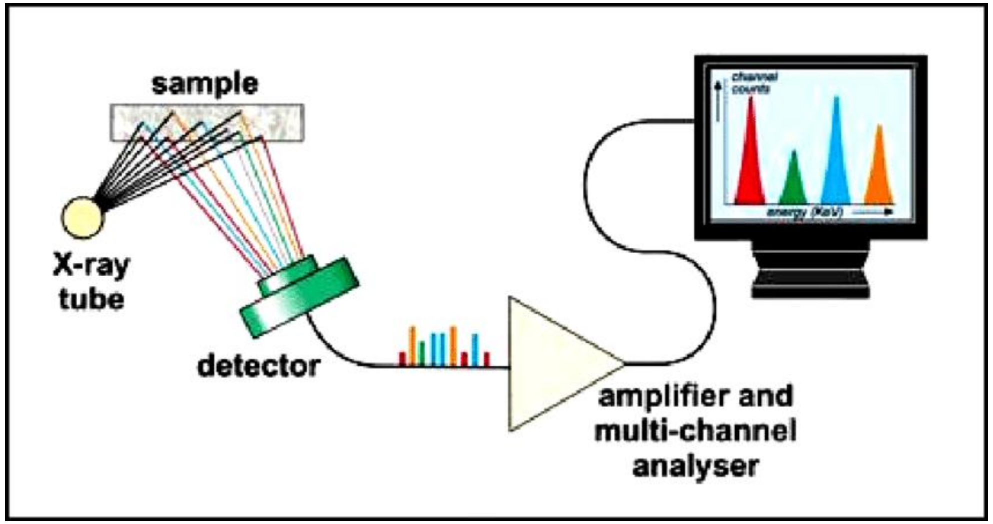

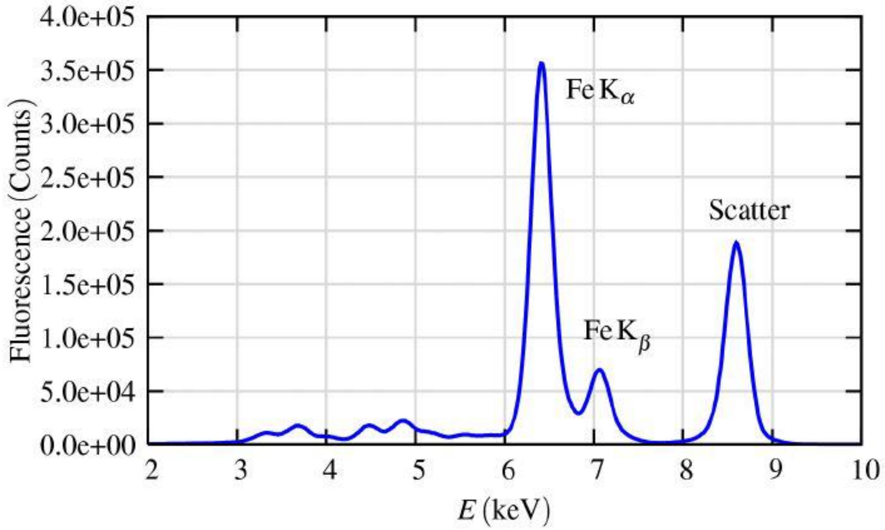

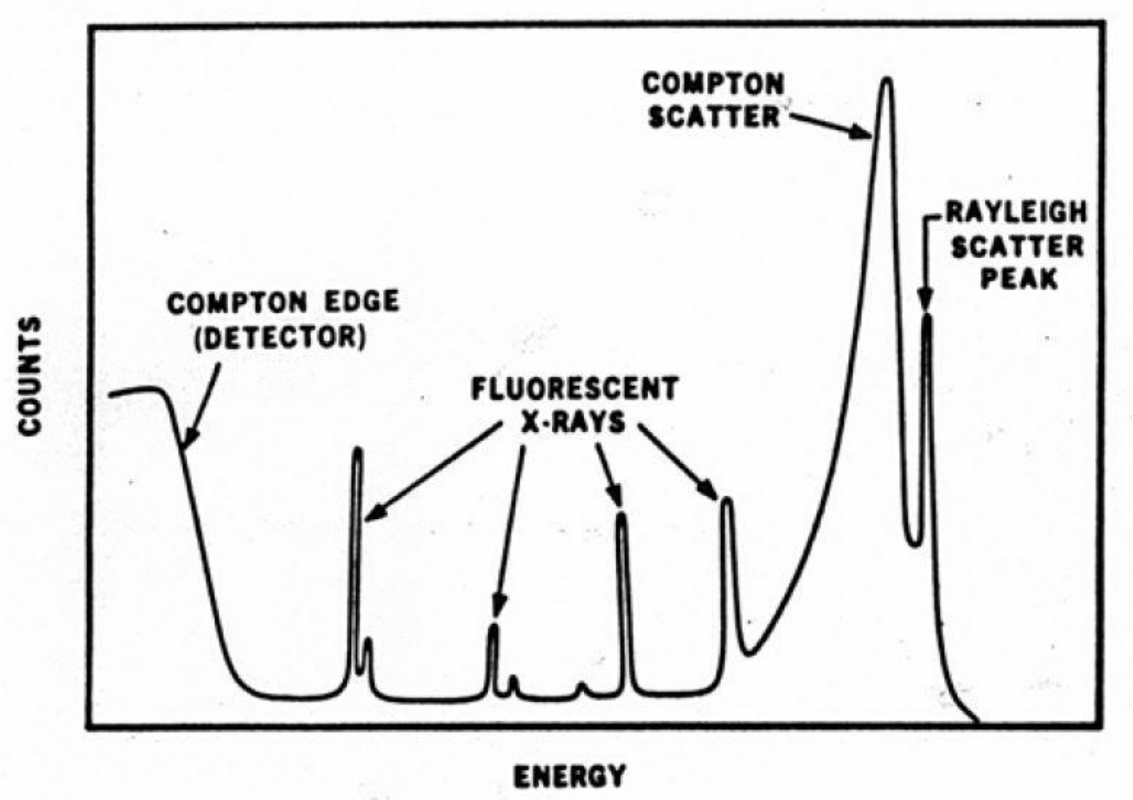

X-ray Absorption Fine Structure (XAFS) spectroscopy and XANES (X-ray Absorption Near Edge Structure)

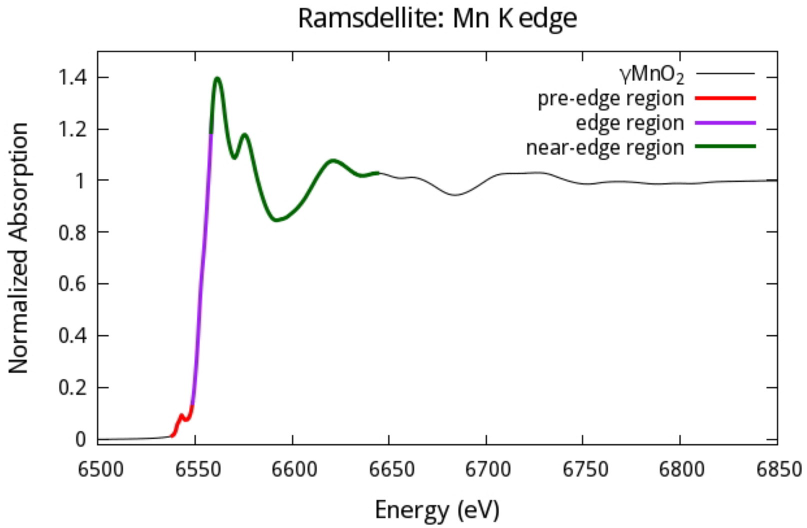

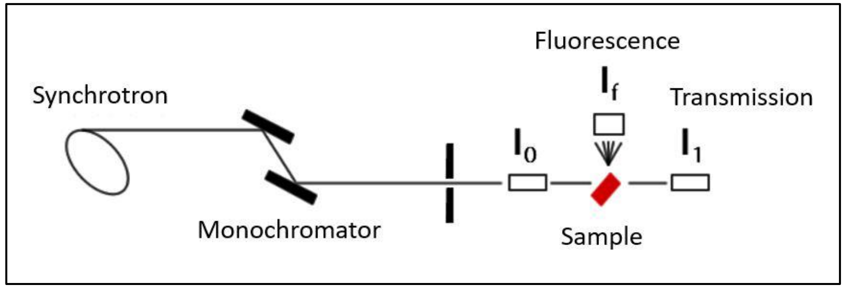

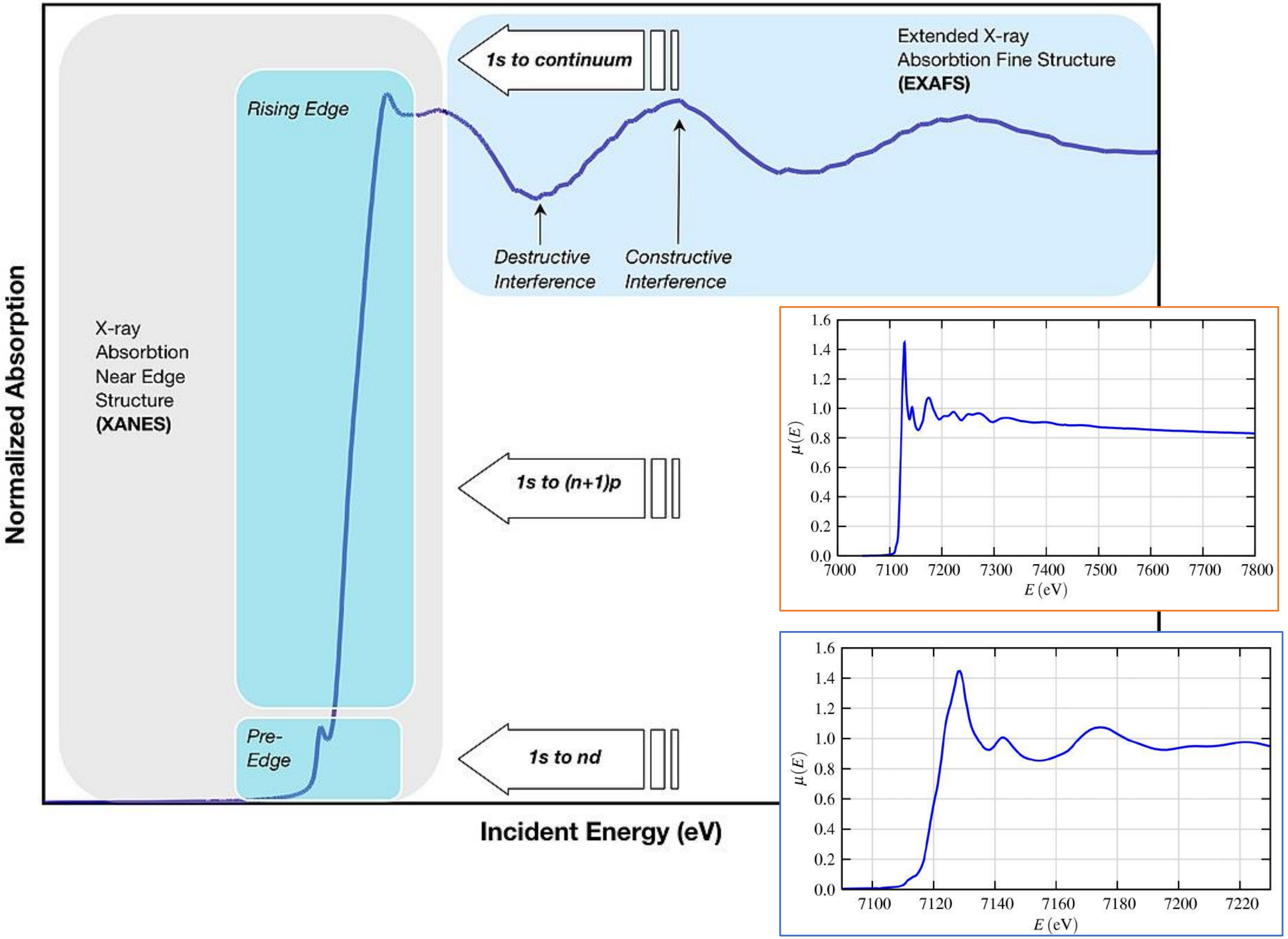

Why design a new detector system?

Requirements of the beamline scientist:

- Very good energetic resolution
- Work at room temperature or moderate cooling
- Large area, in multipixel array
- Low dead time
- High count rate
- Reliability and repeatability
- Excellent interaction with beamline software
- Ease of use by users (error-proof)
- Customized system geometry and features

Evolution of the Detector System (1)

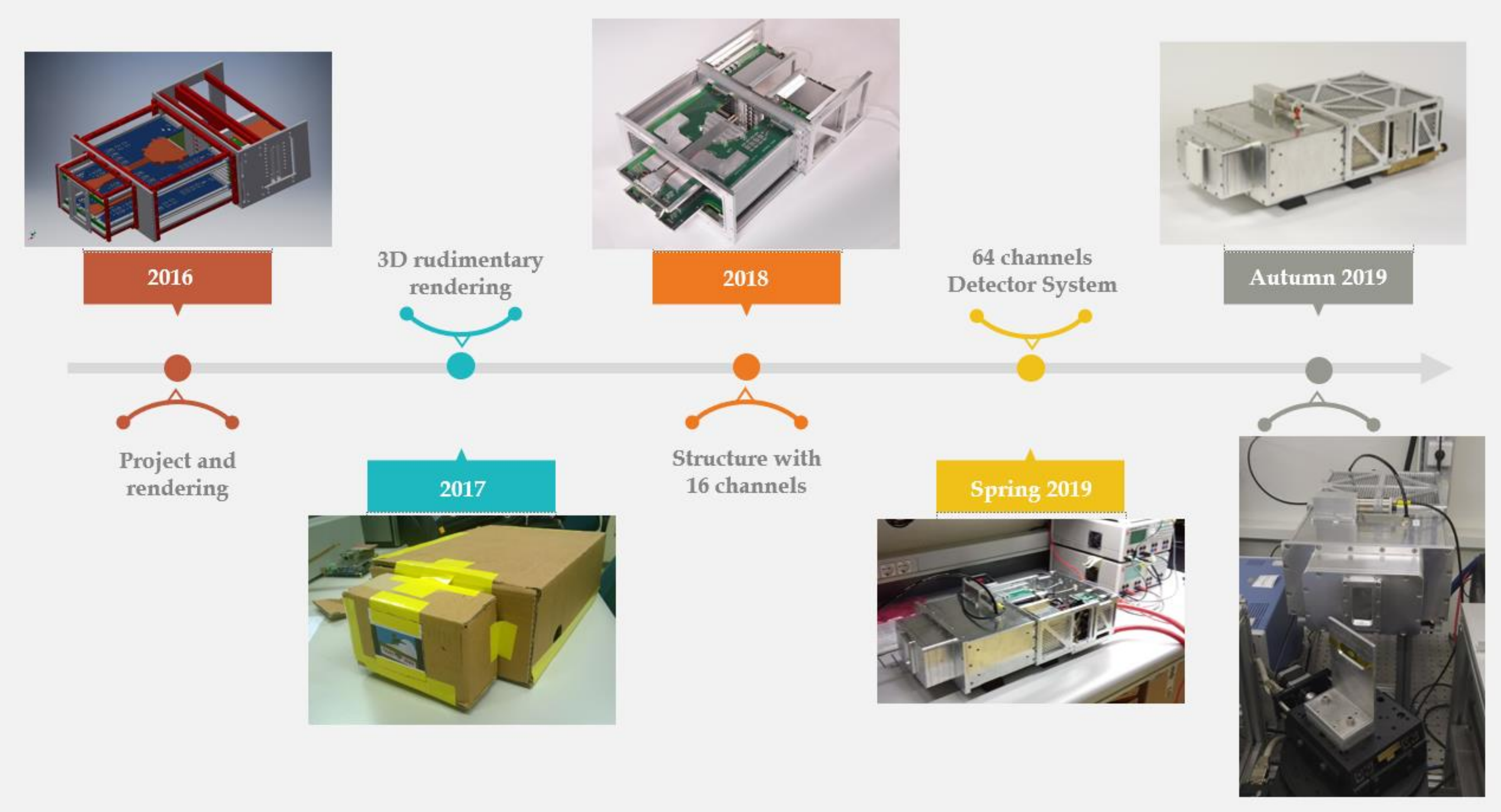

Section of SDD sensor and potential energy of the electrons

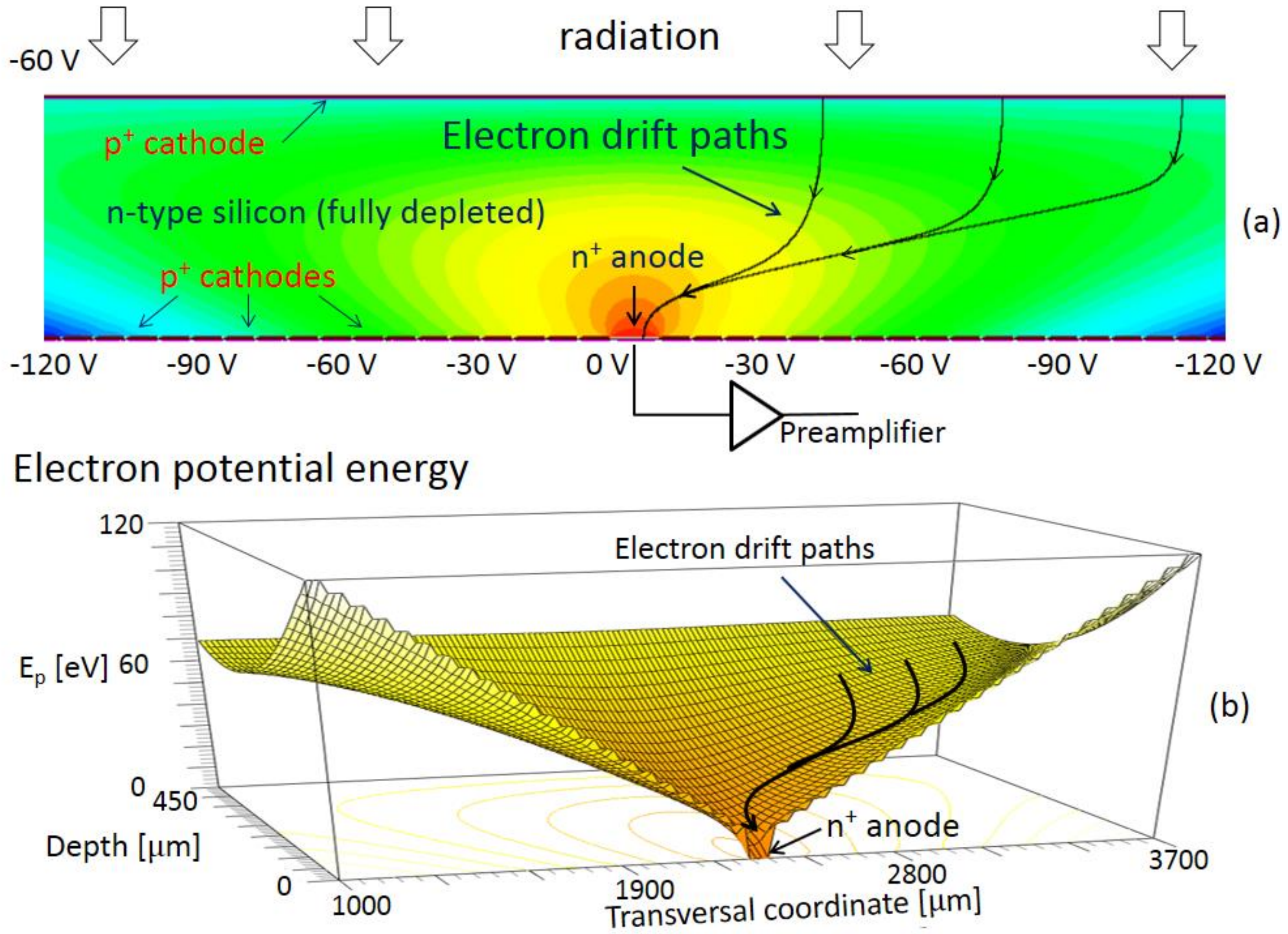

Wafer ReDSoX - SDD

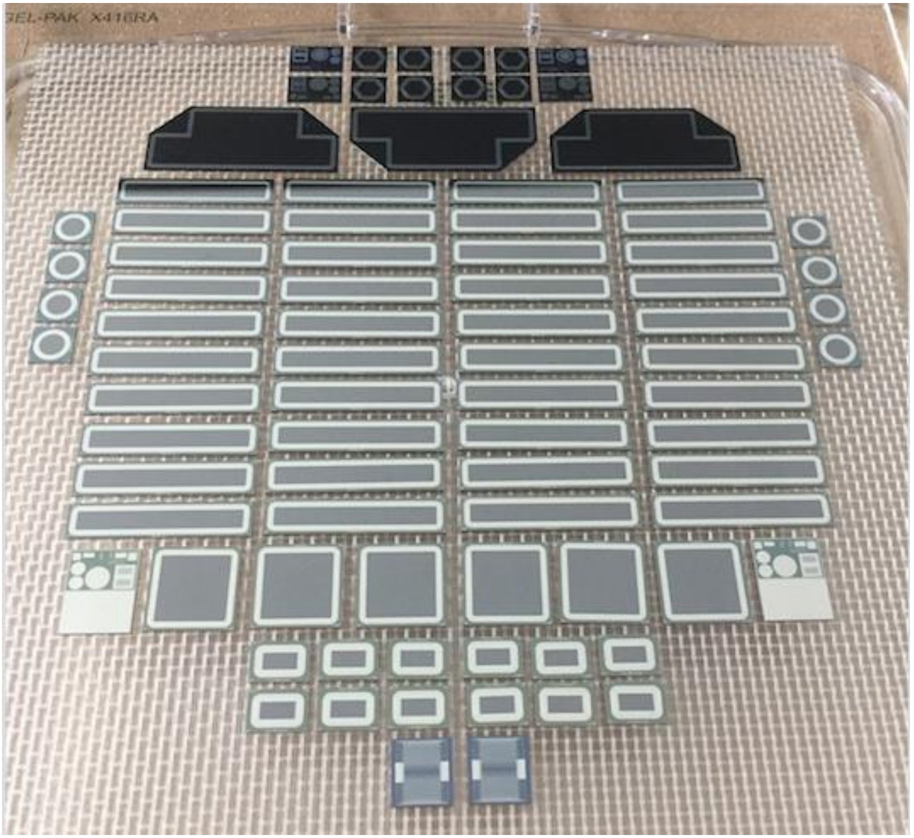

G. Bertuccio, et al., IEEE TRANSACTIONS ON NUCLEAR SCIENCE, VOL. 63, NO. 1, FEBRUARY 2016

SIRIO: Ultra Low Noise CMOS Charge Sensitive Preamplifier

Very-low leakage current production process was developed at FBK

- Typical: < 150 pA/cm²
- Minimum: 25 pA/cm²

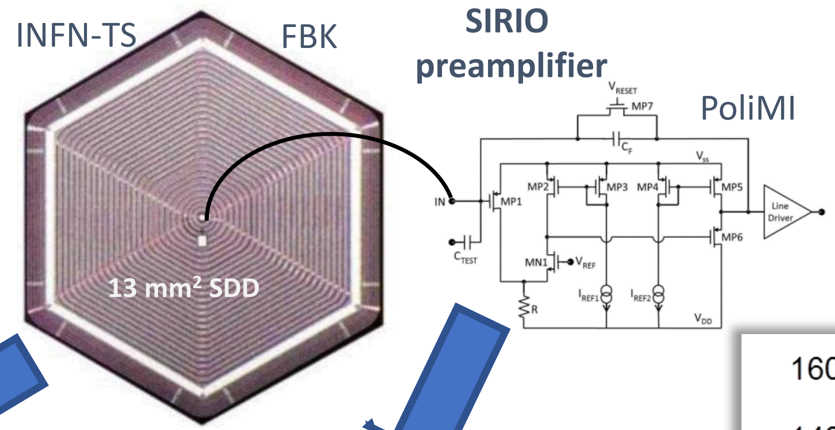

Low-power and very-low noise optimized preampl. in sub-micron technology

- Power: 10 mW including the output buffer
- ENC of 1.27 e⁻ r.m.s. at 20 °C

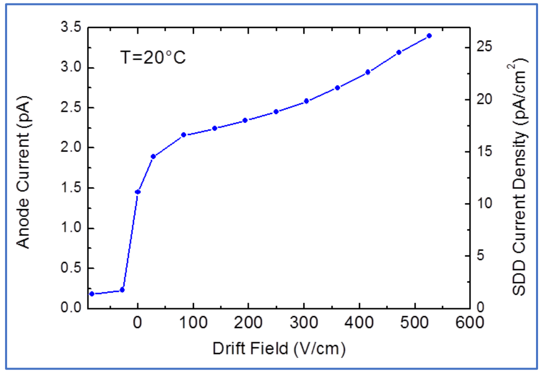

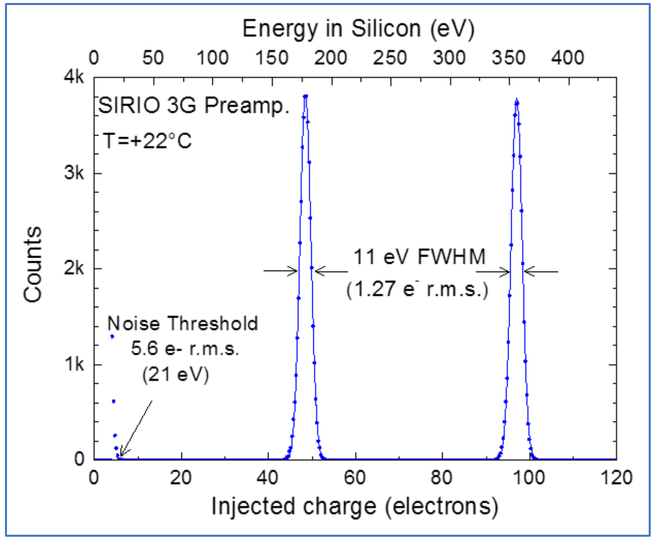

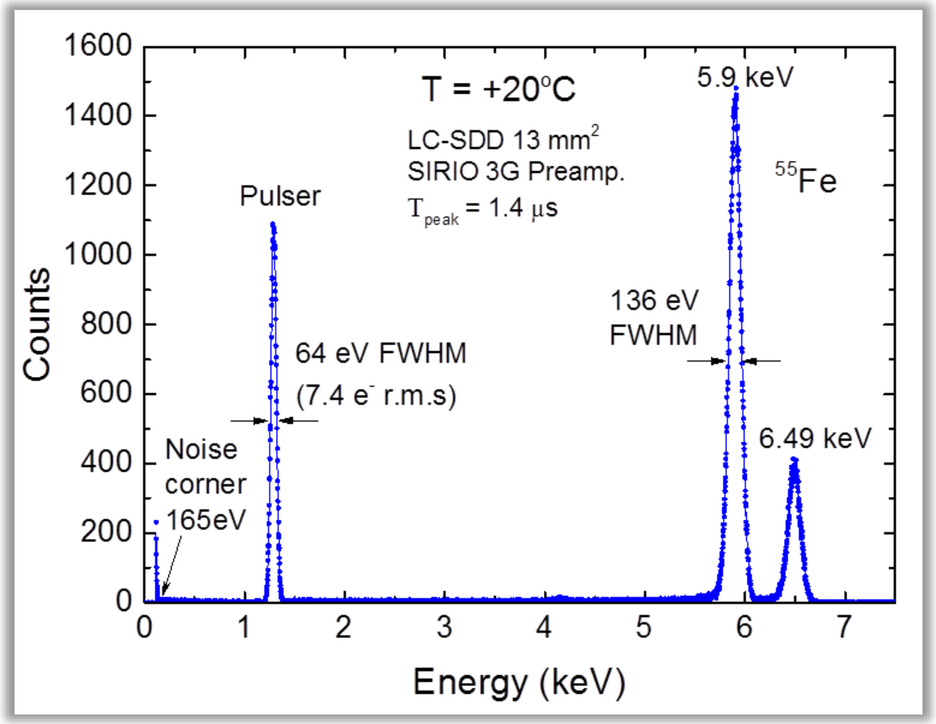

G. Bertuccio, et al., IEEE TRANSACTIONS ON NUCLEAR SCIENCE, VOL. 63, NO. 1, FEBRUARY 2016

Sensor and preamplificator

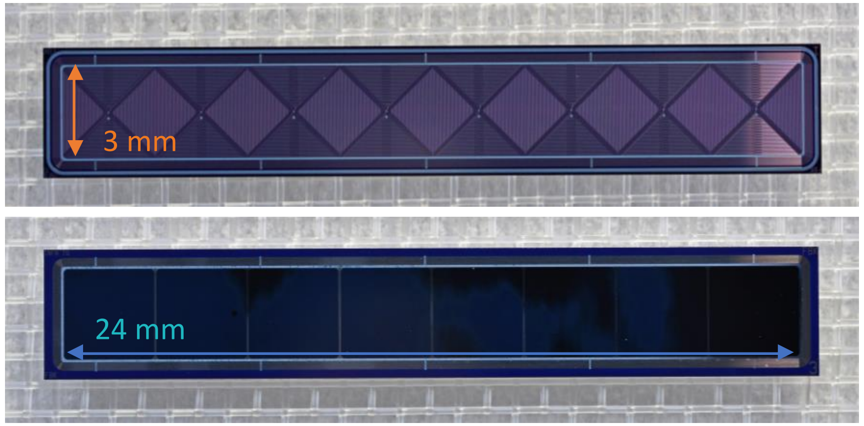

- Sensors: SDD (linear array comprising 8 square cells with a 3 x 3 mm^2 active area)
- **64 channels -> 576 mm^2 active area**
- Preamplifier: SIRIO (SFS3)
- Detector PCB

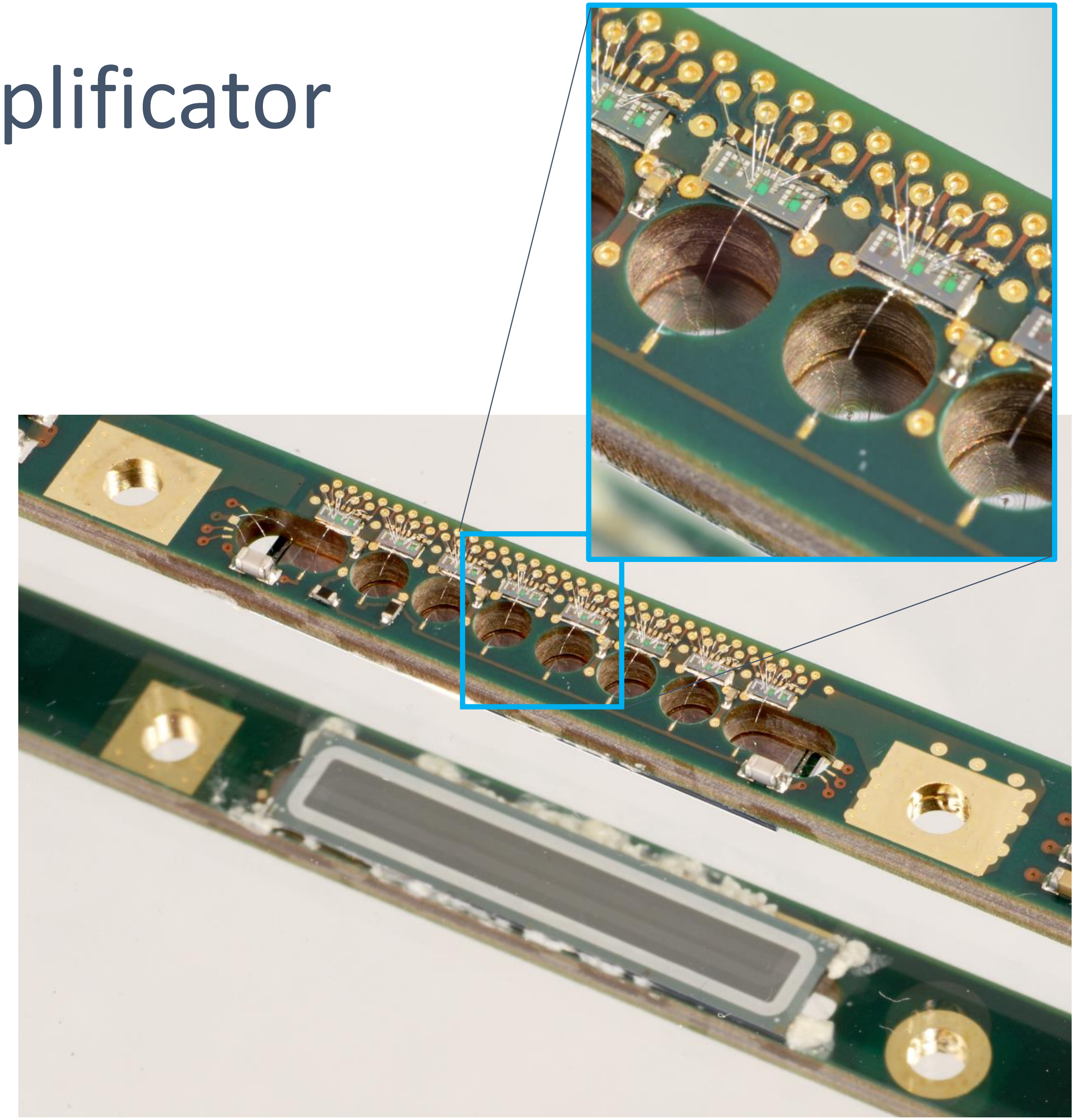

Scheme of the Detector System

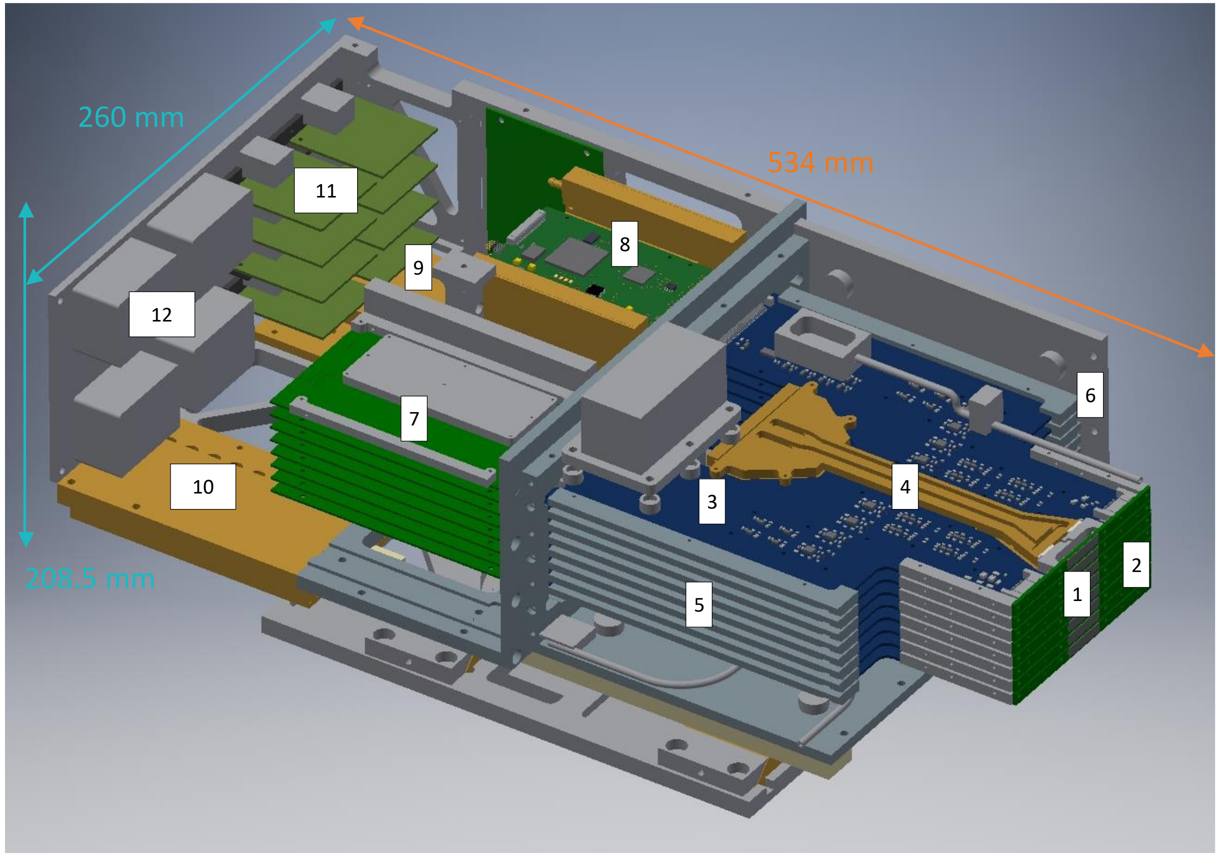

1. Sensors
2. Detector PCBs
3. Front-End PCBs
4. Brass profile with cooling liquid flowing inside
5. Insertion guides at flanks of detecting heads
6. Rails for eight detection heads
7. Power supply and filters PCBs
8. Back-End PCBs
9. Cooling distribution inlet
10. Cooling distribution outlet
11. Ethernet PCBs
12. Power supply connectors

Comparison of characteristics and performance between the new detection system based on Silicon Drift Detectors of XAFS beamline of Elettra and SESAME

D. Cirrincione

FICUS software

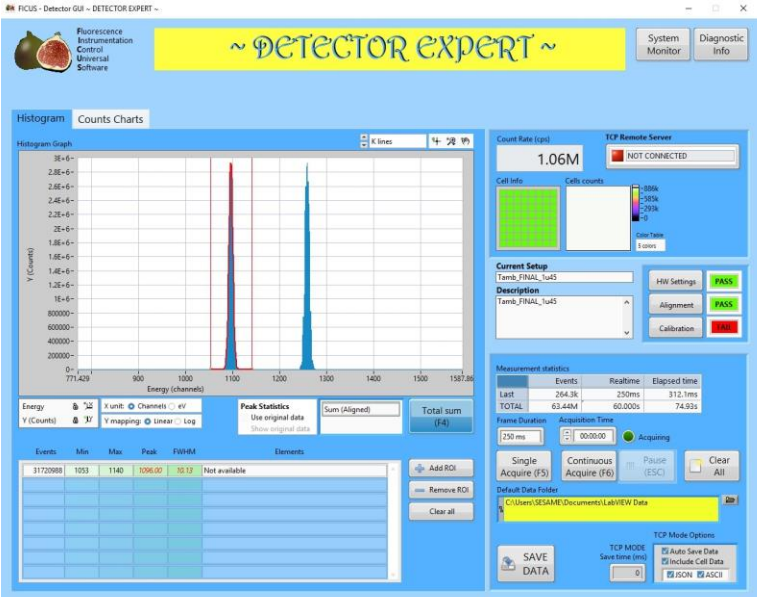

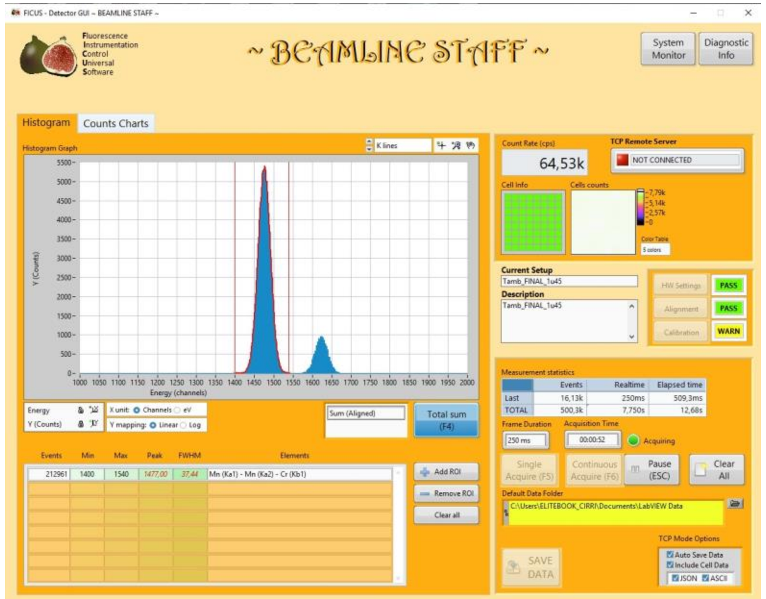

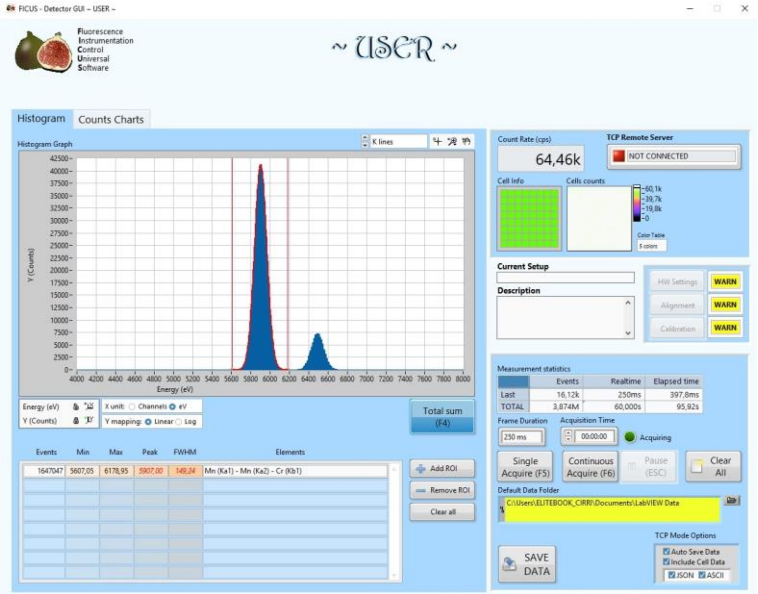

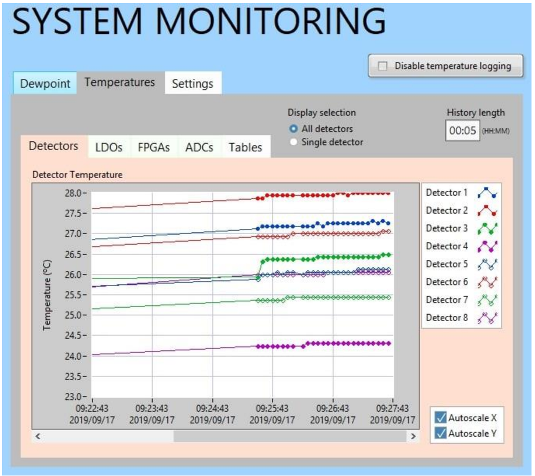

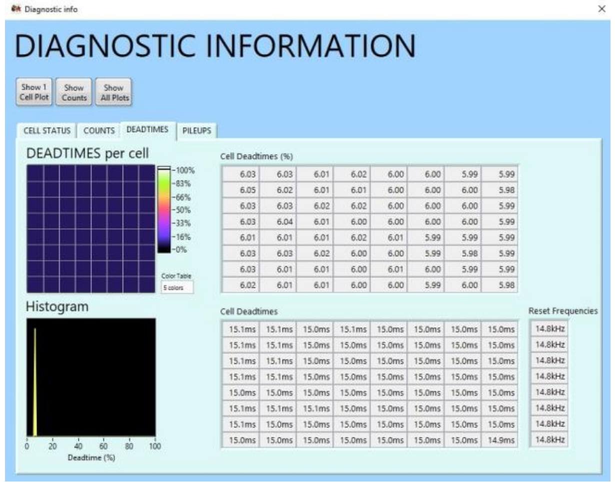

The Detector System

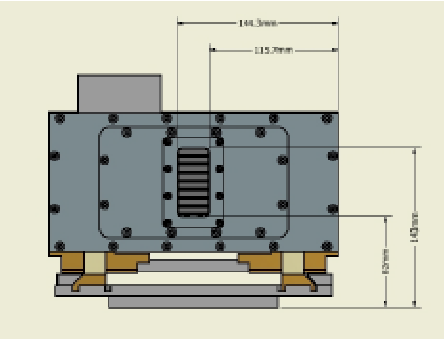

Figure 9: Front side of the detector system

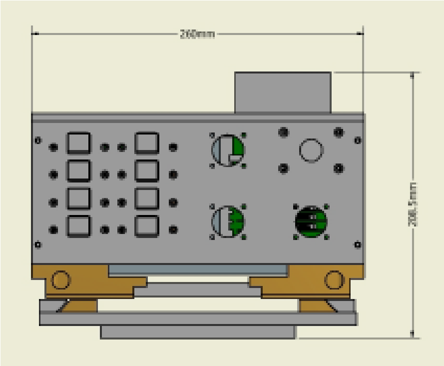

Figure 10: Back side of the detector system

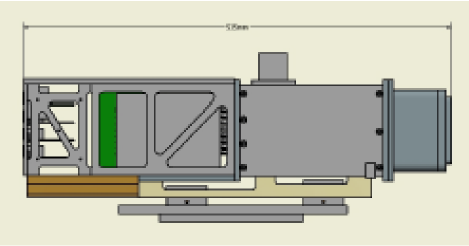

Figure 11: Right side of the detector system

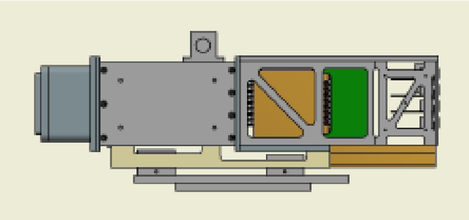

Figure 12: Left side of the detector system

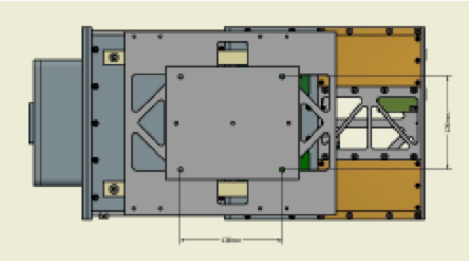

Figure 13: Down side of the detector system

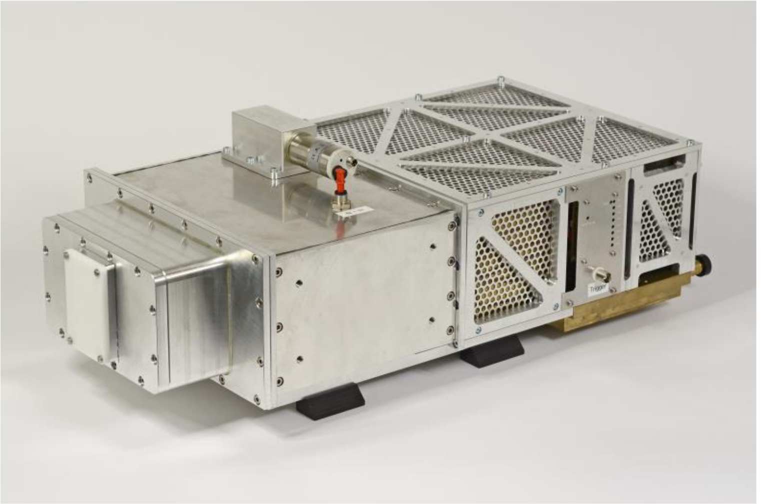

The Detector System

- **8 strips**
- **64 channels**
- **576 mm² active area**
- **[500 mm² collimated active area for DS2]**

- **Tamb**: stabilization of temperature (nitrogen flushing, chiller set at 20 °C and peltier cells at 0.3 V)
- **Tcool**: stabilization of temperature (nitrogen flushing, chiller set at 20 °C and peltier cells at 2.0 V)

- **Calibration sample:** K, Ti, Mn, Zn, Br, Zr

DS2 -> Difference between the two version

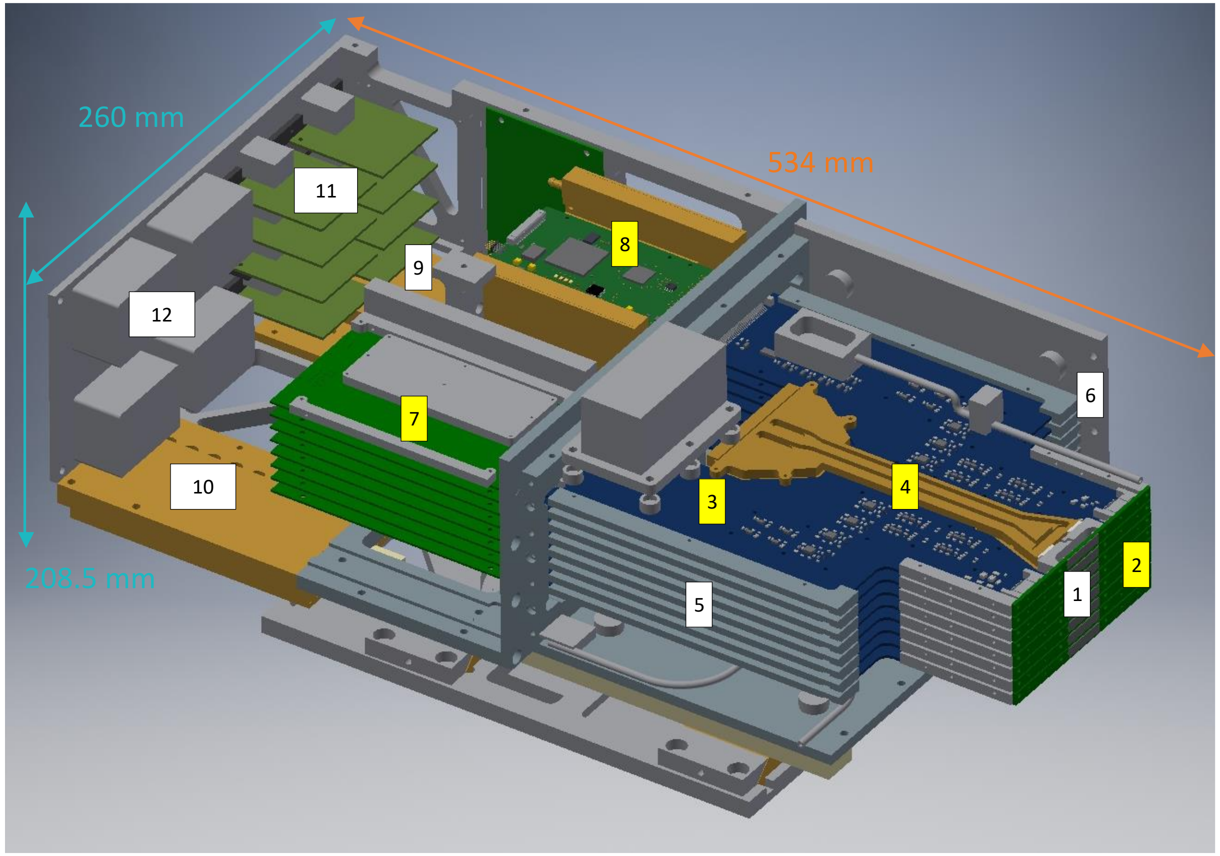

1. Sensors and collimators
2. Detector PCBs
3. Front-End PCBs
4. Brass profile with cooling liquid flowing inside
5. Insertion guides at flanks of detecting heads
6. Rails for eight detection heads
7. Power supply and filters PCBs
8. Back-End PCBs (FIR)
9. Cooling distribution inlet
10. Cooling distribution outlet
11. Ethernet PCBs
12. Power supply connectors
13. FICUS software (alignment, calibration, tools)
14. Digital filters

D2: features with or without collimators

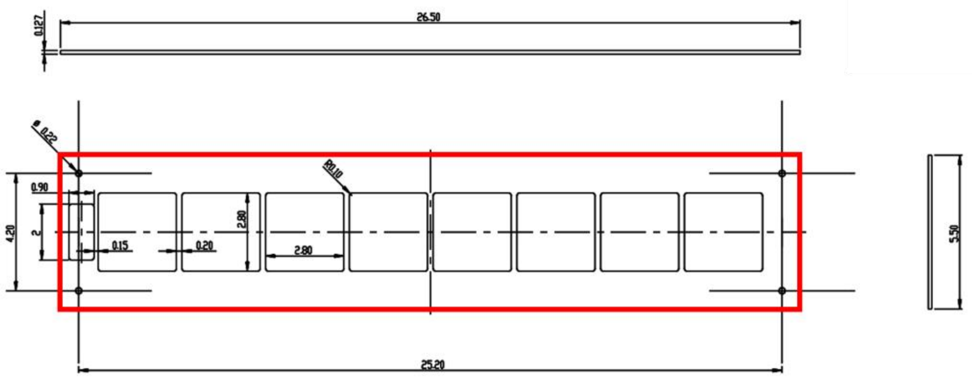

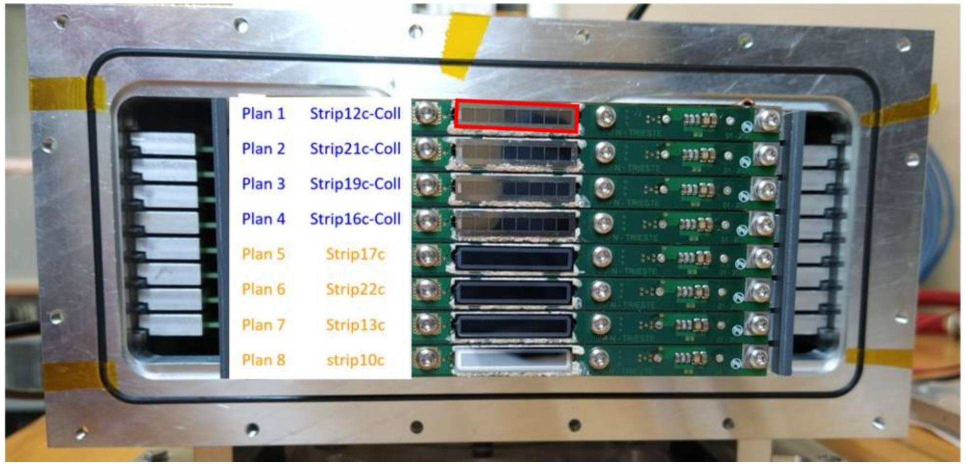

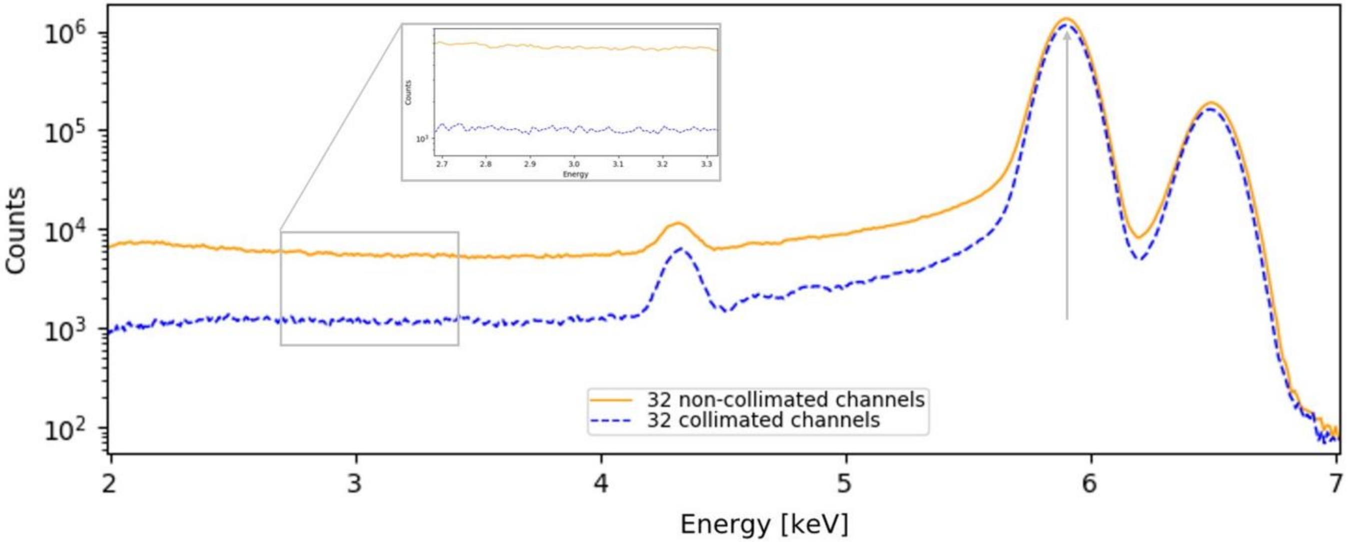

	32 collimated channels	32 non-collimated channels
Part of the detector system	top	bottom
Average temperature of the sensors	23 °C	23 °C
FWHM at the Mn 5.9 Kα line	174 eV	178 eV
Best channel - FWHM	159 eV	166 eV
Worst channel - FWHM	199 eV	211 eV
Acquisition time	30 min	30 min
Counts	23,01 M	29,79 M
Peak to background ratio	972	243

DS2 – setup on XAFS Beamline of Elettra

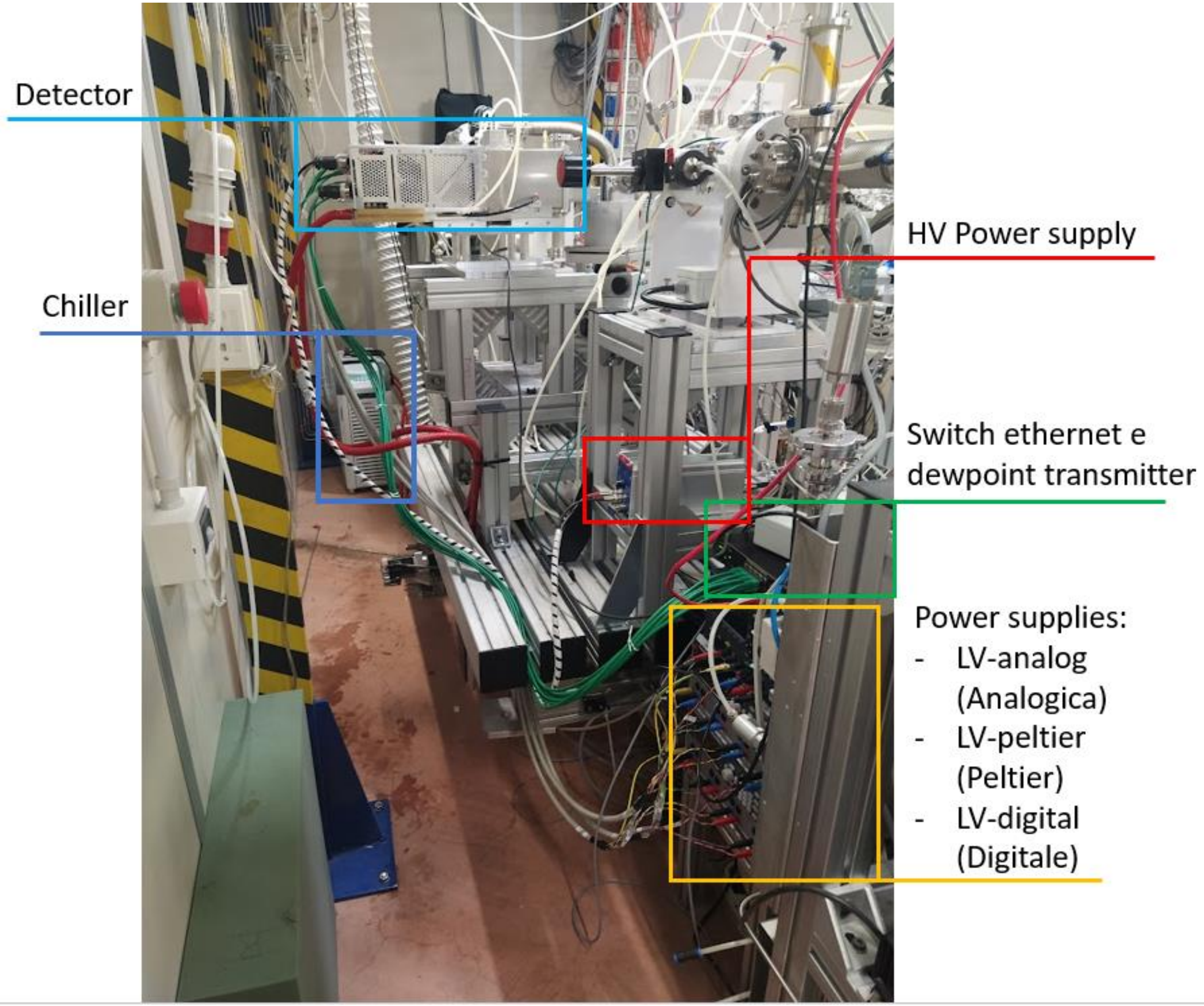

DS1 – setup on XRF/XAFS Beamline of SESAME

Detector

HV Power supply

Power supply:
- LV-analog (Analogica)

Chiller

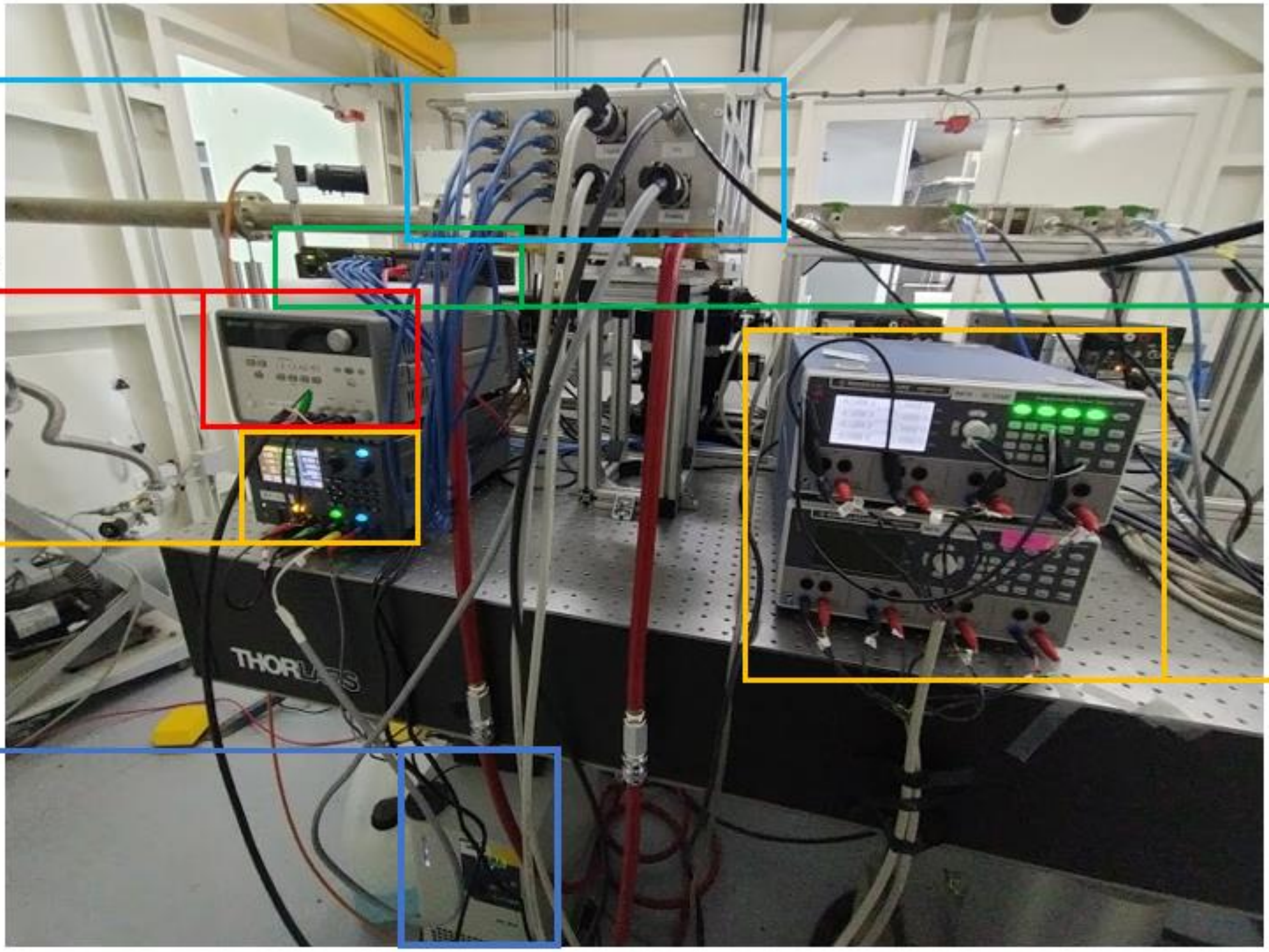

Switch ethernet e dewpoint transmitter

Power supplies:
- LV-peltier (Peltier)
- LV-digital (Digitale)

Test with DS1

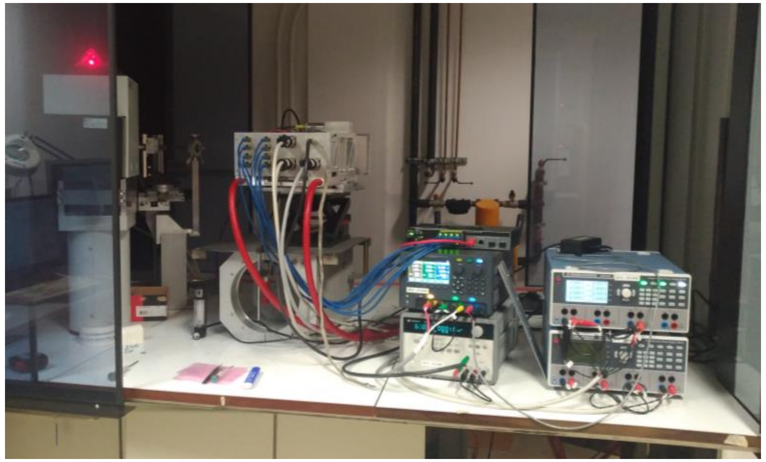

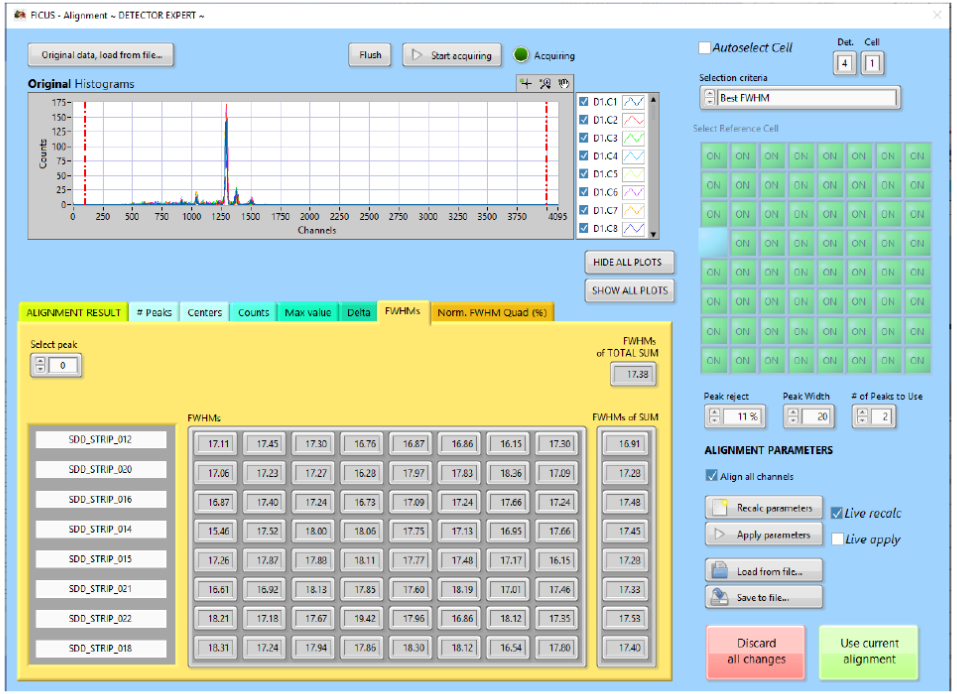

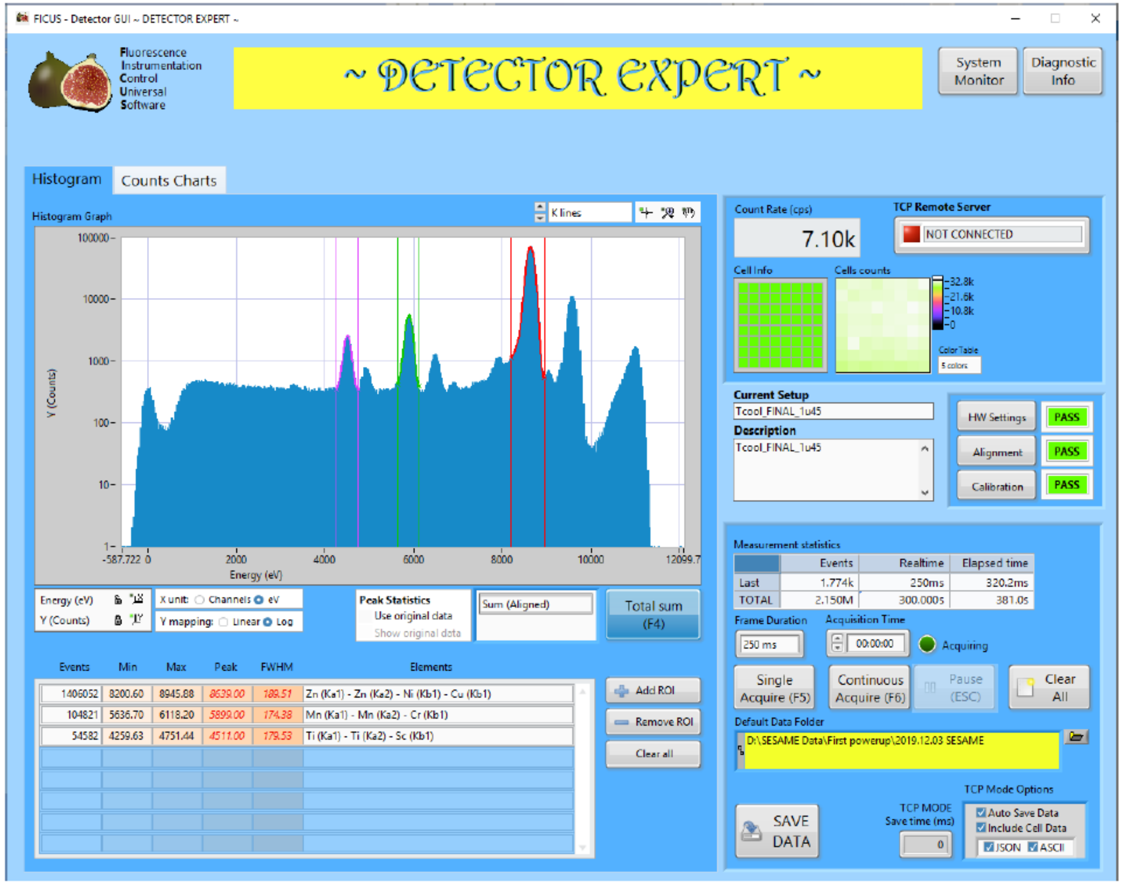

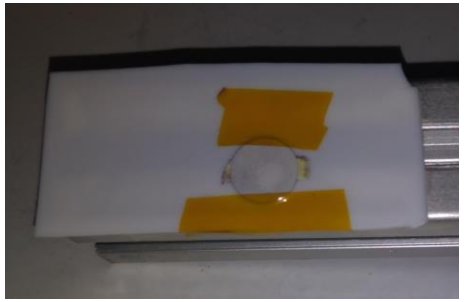

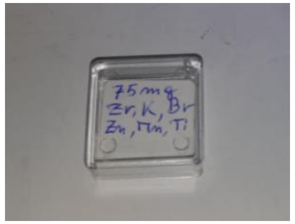

Calibration sample
(Zr, K, Br, Zn, Mn, Ti)

Performance of DS1

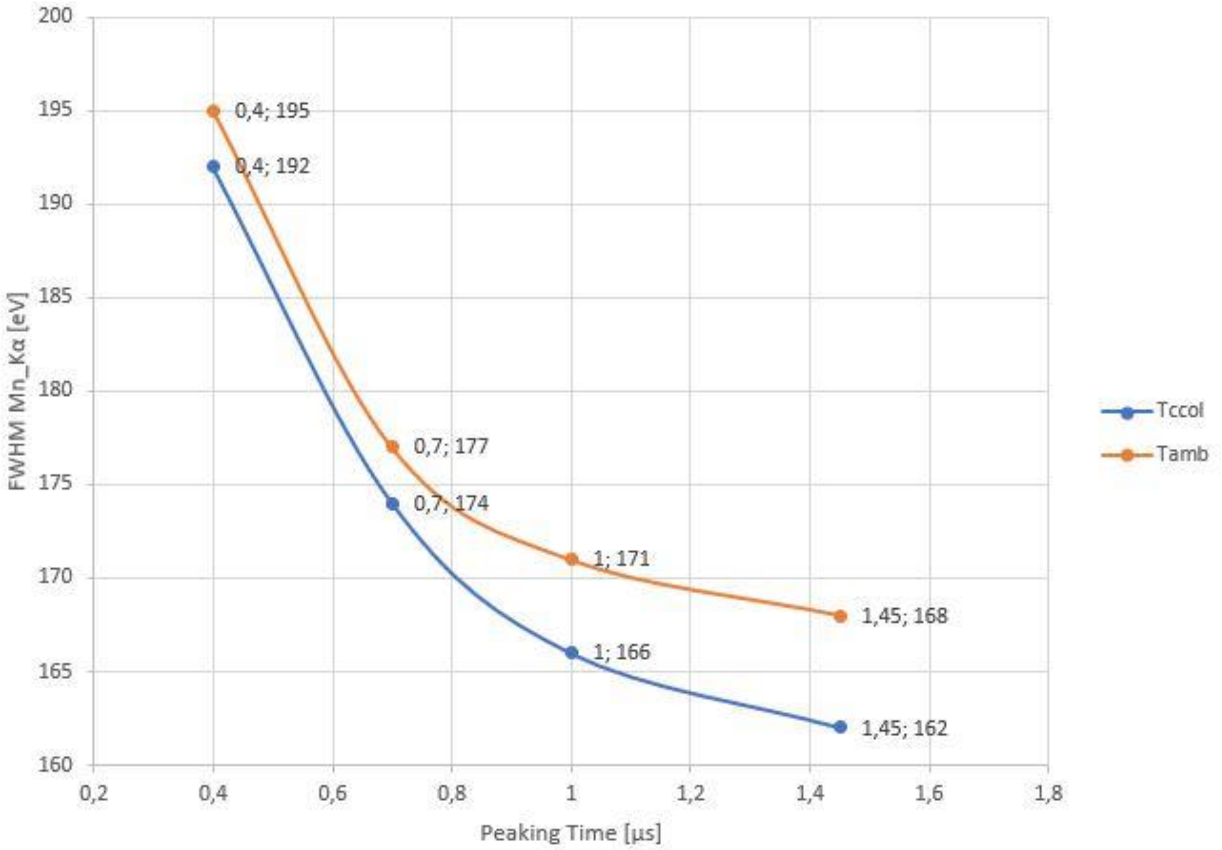

Temperature	FWHM Mn kα [eV]	Peaking time [µs]
Tamb	195	0,4
Tamb	177	0,7
Tamb	171	1,0
Tamb	168	1,45
Tcool	192	0,4
Tcool	174	0,7
Tcool	166	1,0
Tcool	162	1,45

Mode select
Last value

	Detector	LDO	FPGA	ADC
Detector 1	27.81 °C	43.56 °C	35.81 °C	32.06 °C
Detector 2	28.50 °C	43.12 °C	35.87 °C	33.06 °C
Detector 3	27.12 °C	40.50 °C	35.94 °C	32.75 °C
Detector 4	24.75 °C	44.81 °C	36.25 °C	32.87 °C
Detector 5	26.75 °C	42.81 °C	34.75 °C	32.50 °C
Detector 6	27.50 °C	43.25 °C	35.19 °C	31.69 °C
Detector 7	25.87 °C	42.25 °C	35.94 °C	32.06 °C
Detector 8	26.75 °C	42.94 °C	35.25 °C	33.25 °C

Mode select
Last value

	Detector	LDO	FPGA	ADC
Detector 1	7.75 °C	48.00 °C	38.25 °C	33.56 °C
Detector 2	8.37 °C	47.44 °C	38.31 °C	34.69 °C
Detector 3	5.31 °C	44.12 °C	38.12 °C	34.37 °C
Detector 4	3.37 °C	49.00 °C	38.50 °C	34.44 °C
Detector 5	4.94 °C	46.69 °C	36.87 °C	33.81 °C
Detector 6	4.50 °C	47.06 °C	37.75 °C	33.44 °C
Detector 7	5.69 °C	46.25 °C	38.50 °C	33.56 °C
Detector 8	6.56 °C	47.12 °C	37.87 °C	34.75 °C

Performance of DS1 (1.5 μs peaking time, Mn_kα [eV])

Strip Position	Strip Name	Ch1 [eV]	Ch2 [eV]	Ch3 [eV]	Ch4 [eV]	Ch5 [eV]	Ch6 [eV]	Ch7 [eV]	Ch8 [eV]
1	strip12	166	186	166	166	168	167	162	169
2	strip20	167	168	170	161	166	176	167	167
3	strip16	162	163	168	166	172	163	164	161
4	strip14	162	164	169	169	164	163	170	166
5	strip15	165	170	164	169	166	161	163	164
6	strip21	170	167	163	170	165	167	167	165
7	strip22	175	172	170	173	167	168	165	165
8	strip18	180	167	169	174	173	179	168	175

Temperature	FWHM Mn kα [eV]	Peaking time [μs]
Tamb	195	0,4
Tamb	177	0,7
Tamb	171	1,0
Tamb	168	1,45
Tcool	192	0,4
Tcool	174	0,7
Tcool	166	1,0
Tcool	162	1,45

Strip Position	Strip Name	Ch1 [eV]	Ch2 [eV]	Ch3 [eV]	Ch4 [eV]	Ch5 [eV]	Ch6 [eV]	Ch7 [eV]	Ch8 [eV]
1	strip12	160	169	159	158	163	162	155	164
2	strip20	159	164	160	156	162	167	165	160
3	strip16	157	156	160	158	164	156	160	155
4	strip14	156	160	164	165	158	156	158	159
5	strip15	162	166	159	158	161	159	156	158
6	strip21	159	158	158	160	161	165	162	160
7	strip22	161	162	161	174	161	162	160	160
8	strip18	173	165	164	167	166	170	162	171

Mode select
Last value

	Detector	LDO	FPGA	ADC
Detector 1	27.81 °C	43.56 °C	35.81 °C	32.06 °C
Detector 2	28.50 °C	43.12 °C	35.87 °C	33.06 °C
Detector 3	27.12 °C	40.50 °C	35.94 °C	32.75 °C
Detector 4	24.75 °C	44.81 °C	36.25 °C	32.87 °C
Detector 5	26.75 °C	42.81 °C	34.75 °C	32.50 °C
Detector 6	27.50 °C	43.25 °C	35.19 °C	31.69 °C
Detector 7	25.87 °C	42.25 °C	35.94 °C	32.06 °C
Detector 8	26.75 °C	42.94 °C	35.25 °C	33.25 °C

Mode select
Last value

	Detector	LDO	FPGA	ADC
Detector 1	7.75 °C	48.00 °C	38.25 °C	33.56 °C
Detector 2	8.37 °C	47.44 °C	38.31 °C	34.69 °C
Detector 3	5.31 °C	44.12 °C	38.12 °C	34.37 °C
Detector 4	3.37 °C	49.00 °C	38.50 °C	34.44 °C
Detector 5	4.94 °C	46.69 °C	36.87 °C	33.81 °C
Detector 6	4.50 °C	47.06 °C	37.75 °C	33.44 °C
Detector 7	5.69 °C	46.25 °C	38.50 °C	33.56 °C
Detector 8	6.56 °C	47.12 °C	37.87 °C	34.75 °C

DS1 (XANES) sample C09_Cr K-edge

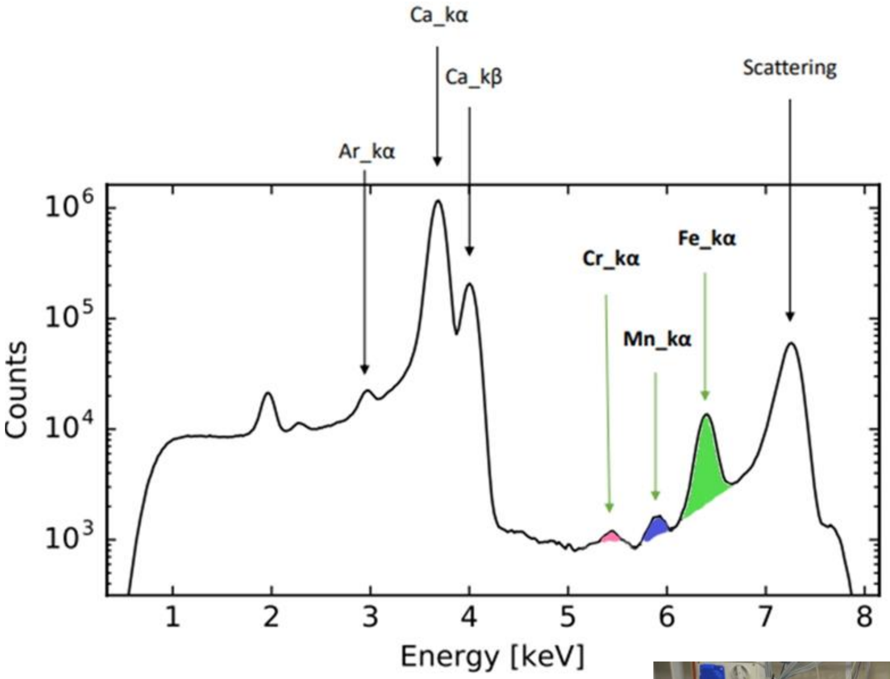

Sample	C09 [mg/kg]	C11 [mg/kg]	C13 [mg/kg]	C20 [mg/kg]
Al	514	300	319	239
V	3.1	2.1	1.2	0.8
Cr	2.90	2.92	3.48	4.48
Fe	397	131	129	212
Mn	38.2	11.9	19.6	12.8
Ni	2.4	1.8	1.6	1.5
Co	1.08	0.58	0.53	0.54
Cu	1.39	0.78	0.82	0.79
Zn	7.3	16.4	11.4	8.4
Rb	0.85	0.52	0.51	0.25
Sr	138	100	105	72
Mo	0.29	0.20	0.16	0.13
Cd	0.18	0.17	0.12	0.34
Ba	6.2	4.2	3.4	3.0
Pb	0.9	2.5	0.8	0.6
U	1.6	1.4	1.3	1.2

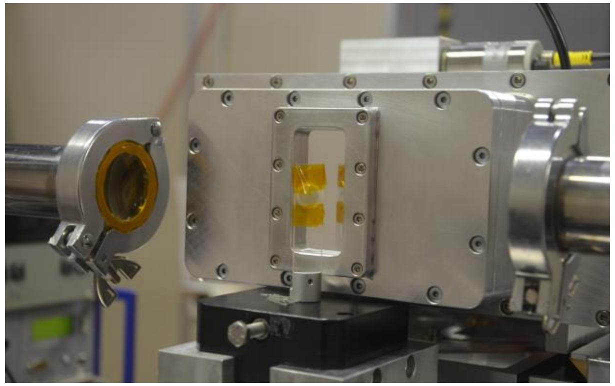

Geological samples

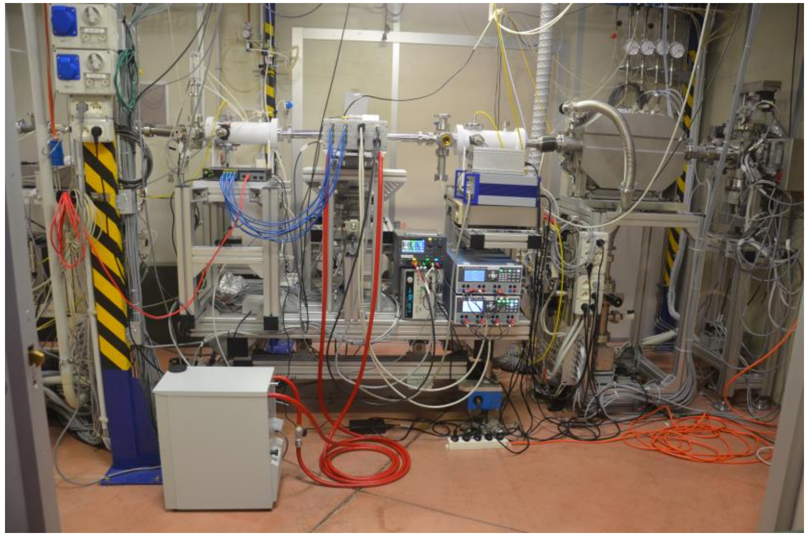

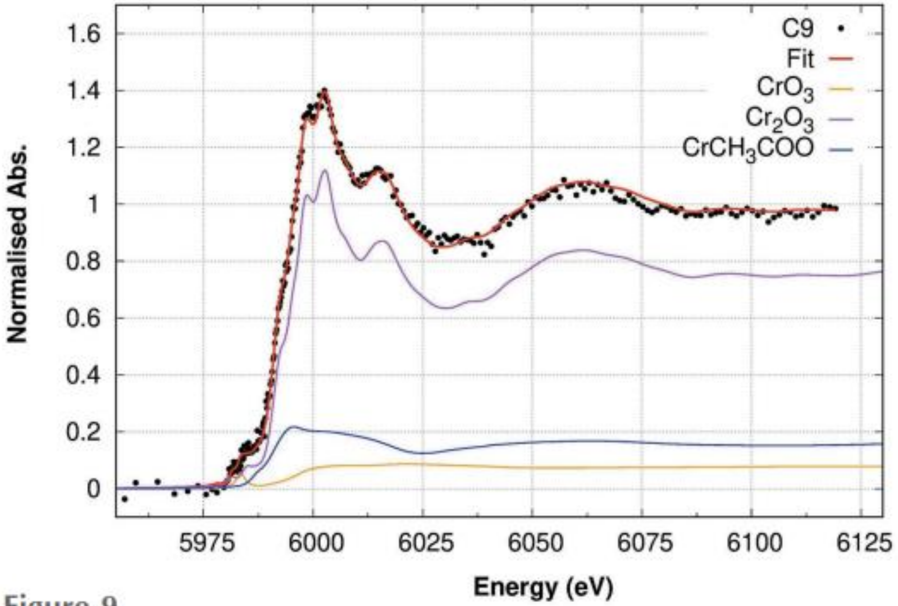

Figure 9
LCA results for sample C9 (Cr concentration = 2.9 p.p.m.) at the Cr *K*-edge. The best fit (red line) to the experimental data (black dots) is obtained by a linear combination of the different phases, reported in the plot according to their multiplicative coefficients.

Carlomagno, Ilaria, et al. "Trace-element XAFS sensitivity: a stress test for a new XRF multi-detector." *Journal of Synchrotron Radiation* 28.6 (2021): 1811-1819.

Comparison of characteristics and performance between the new detection system based on Silicon Drift Detectors of XAFS beamline of Elettra and SESAME

D. Cirrincione

Test with DS2

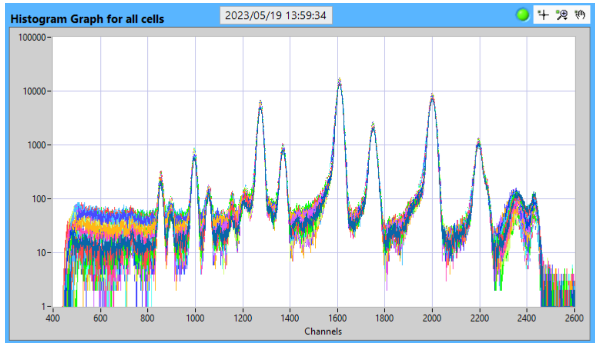

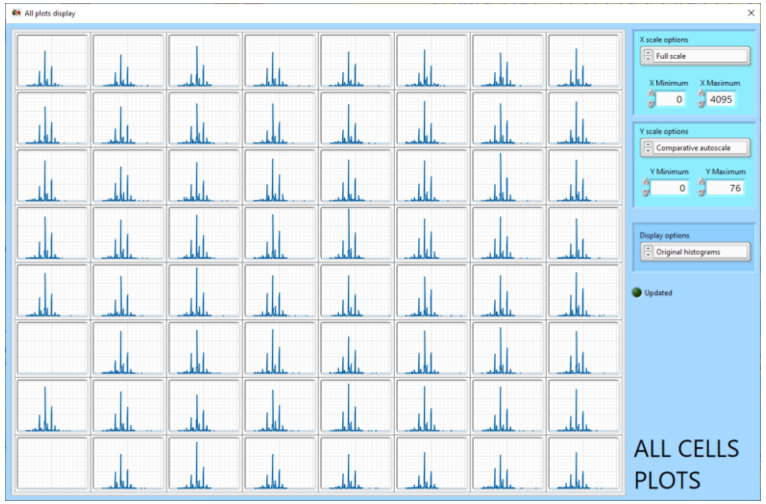

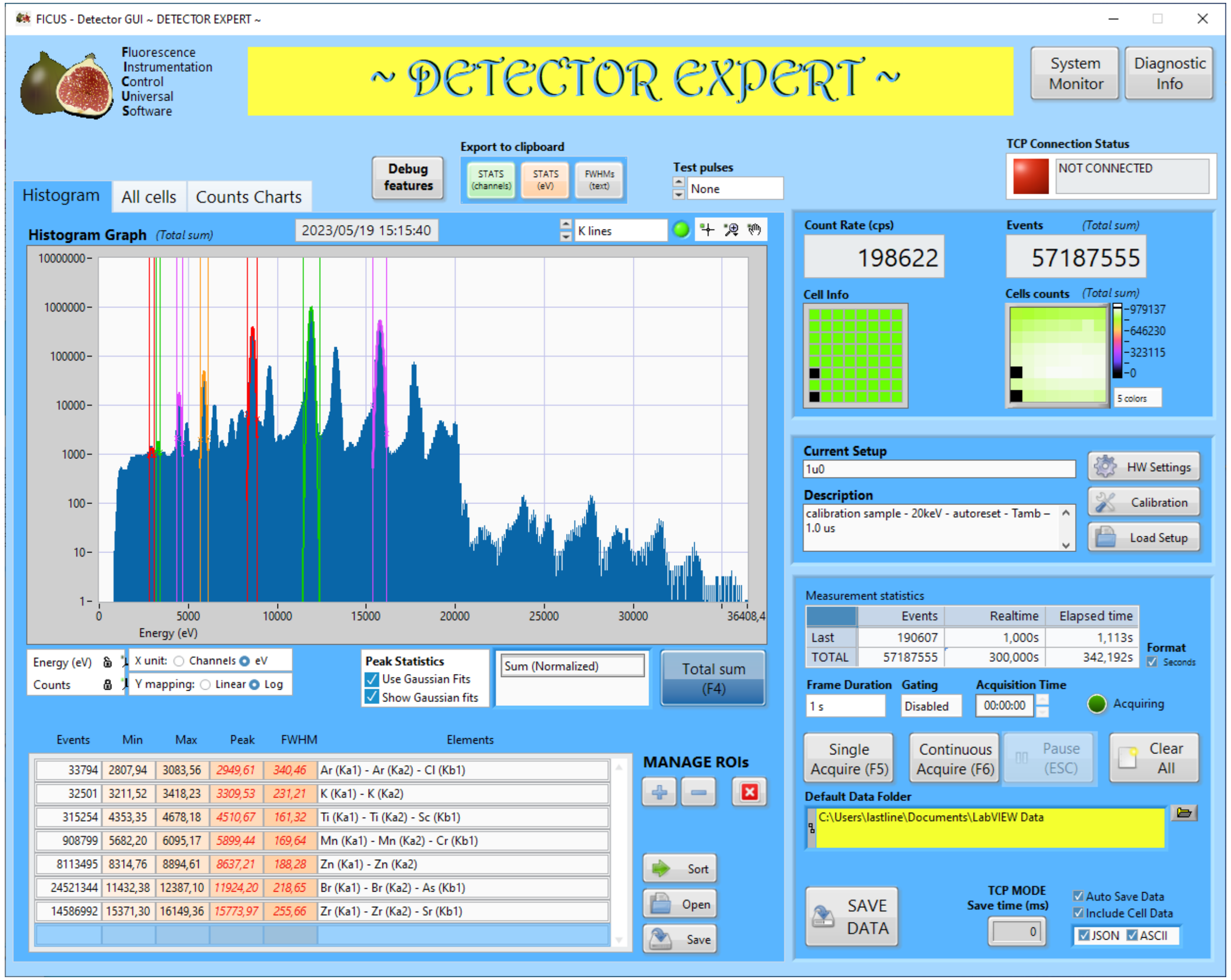

Performance of DS2

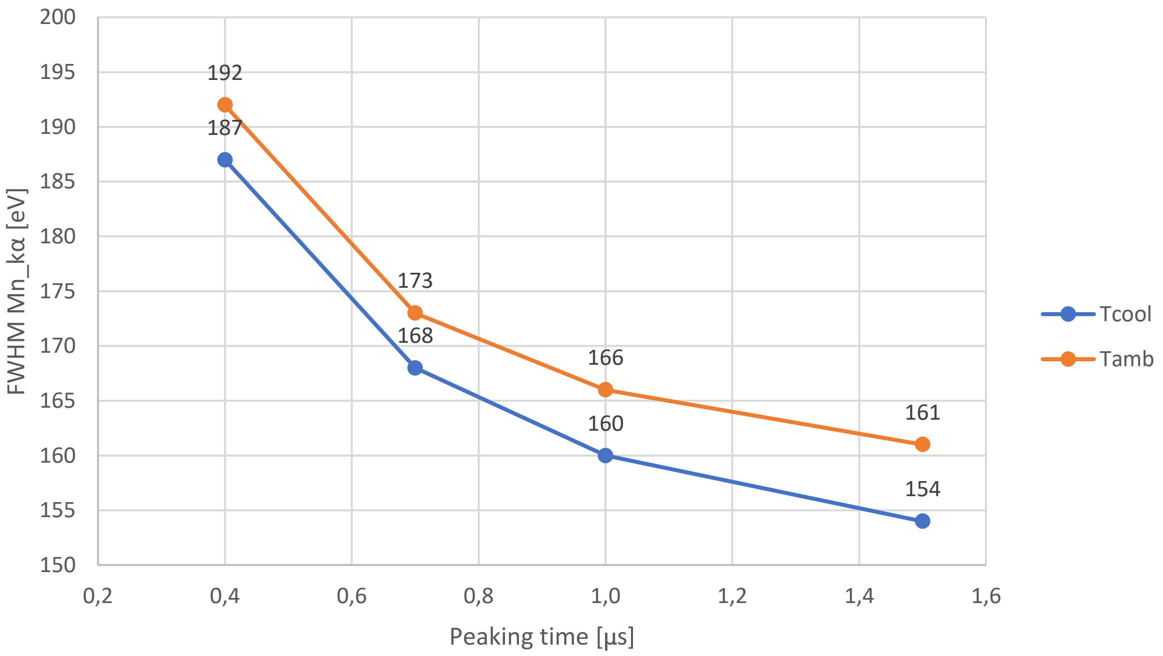

Temperature	FWHM Mn kα [eV]	Peaking time [µs]
Tamb	192	0,4
Tamb	173	0,7
Tamb	166	1
Tamb	161	1,5
Tcool	187	0,4
Tcool	168	0,7
Tcool	160	1
Tcool	154	1,5

- Tamb: medium temperature 26,3 °C
- Tcool: medium temperature 7,4 °C

Performance of DS1

Temperature	FWHM Mn kα [eV]	Peaking time [µs]
Tamb	195	0,4
Tamb	177	0,7
Tamb	171	1,0
Tamb	168	1,45
Tcool	192	0,4
Tcool	174	0,7
Tcool	166	1,0
Tcool	162	1,45

Performance of DS2 (1.5 µs peaking time, Mn_kα [eV])

1u5 - Tamb	ch1	ch2	ch3	ch4	ch5	ch6	ch7	ch8
strip12c	163	168	168	170	166	166	169	166
strip21c	155	164	154	156	166	171	158	159
strip19c	166	159	159	166	162	162	163	163
strip16c	153	153	153	151	155	154	156	157
strip22c	159	168	155	155	166	157	158	156
strip15c	-	160	158	159	151	161	164	157
strip13c	164	165	175	161	162	166	170	165
strip10c	-	179	176	180	181	178	180	173

Temperature	FWHM Mn kα [eV]	Peaking time [µs]
Tamb	192	0,4
Tamb	173	0,7
Tamb	166	1
Tamb	161	1,5
Tcool	187	0,4
Tcool	168	0,7
Tcool	160	1
Tcool	154	1,5

1u5 - Tcool	ch1	ch2	ch3	ch4	ch5	ch6	ch7	ch8
strip12c	157	162	162	167	164	161	162	159
strip21c	149	157	152	148	158	165	151	156
strip19c	158	153	154	157	155	155	160	153
strip16c	147	150	147	147	149	150	151	150
strip22c	151	156	149	149	155	152	152	150
strip15c	-	151	153	151	152	156	157	153
strip13c	158	158	166	158	157	156	163	157
strip10c	-	175	173	177	180	175	177	169

- Tamb: medium temperature 26,3 °C
- Tcool: medium temperature 7,4 °C

Comparison DS1 vs DS2 (XANES) sample C09_Cr K-edge

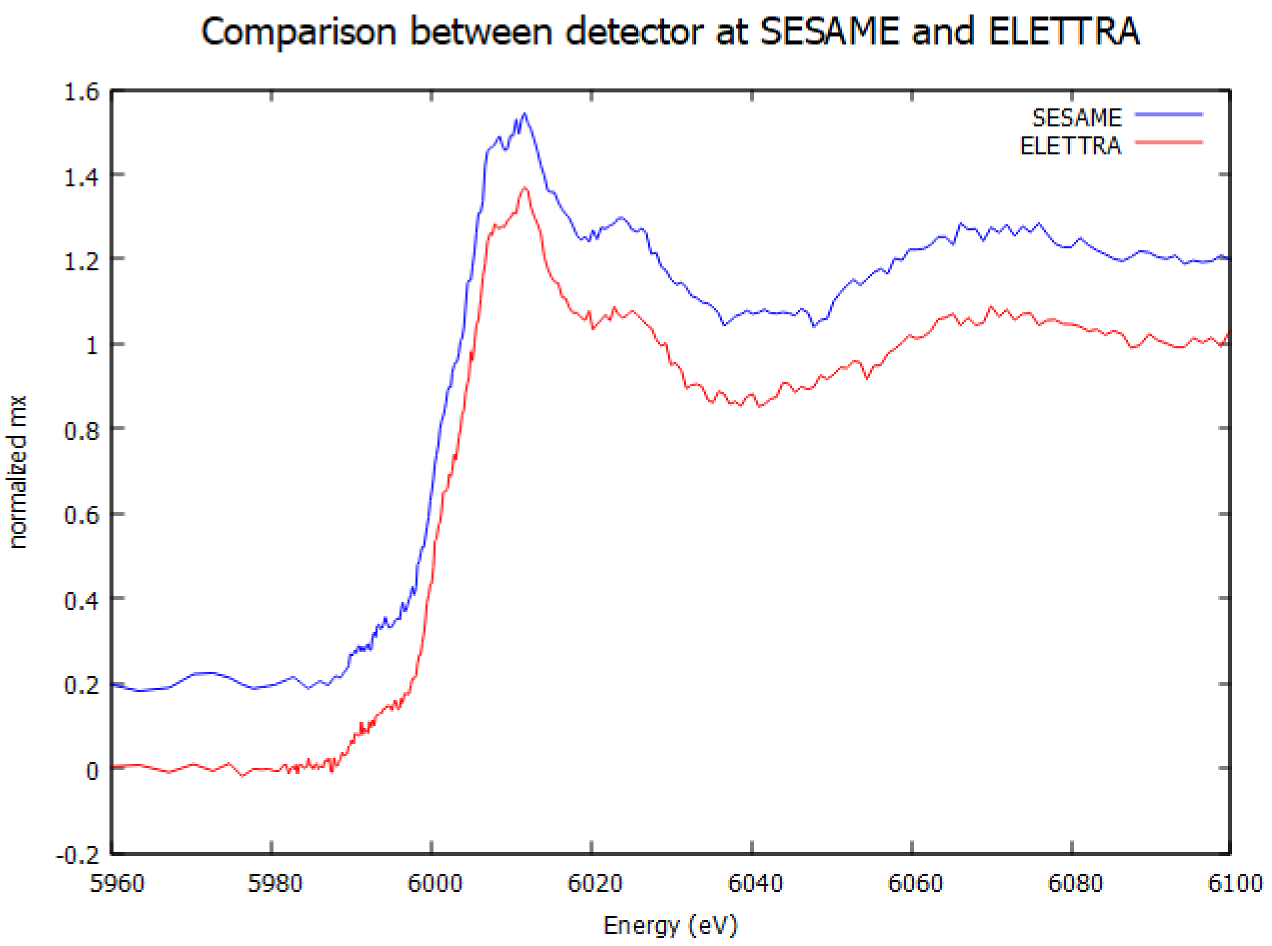

Sample	C09 [mg/kg]	C11 [mg/kg]	C13 [mg/kg]	C20 [mg/kg]
Al	514	300	319	239
V	3.1	2.1	1.2	0.8
Cr	2.90	2.92	3.48	4.48
Fe	397	131	129	212
Mn	38.2	11.9	19.6	12.8
Ni	2.4	1.8	1.6	1.5
Co	1.08	0.58	0.53	0.54
Cu	1.39	0.78	0.82	0.79
Zn	7.3	16.4	11.4	8.4
Rb	0.85	0.52	0.51	0.25
Sr	138	100	105	72
Mo	0.29	0.20	0.16	0.13
Cd	0.18	0.17	0.12	0.34
Ba	6.2	4.2	3.4	3.0
Pb	0.9	2.5	0.8	0.6
U	1.6	1.4	1.3	1.2

Two Detector System for two Synchrotron

SESAME

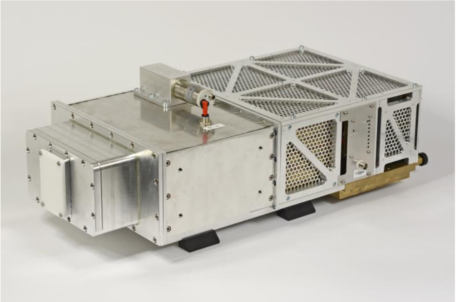

Elettra Sincrotrone Trieste

New beamline, new challenges: TwinMic Beamline (Elettra-Sincrotrone Trieste)

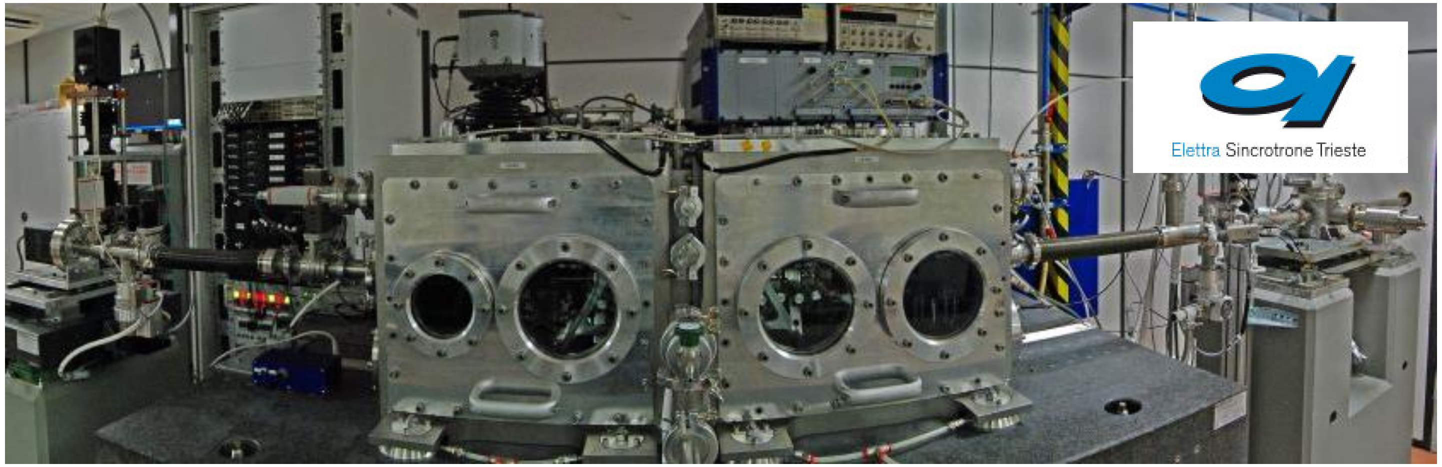

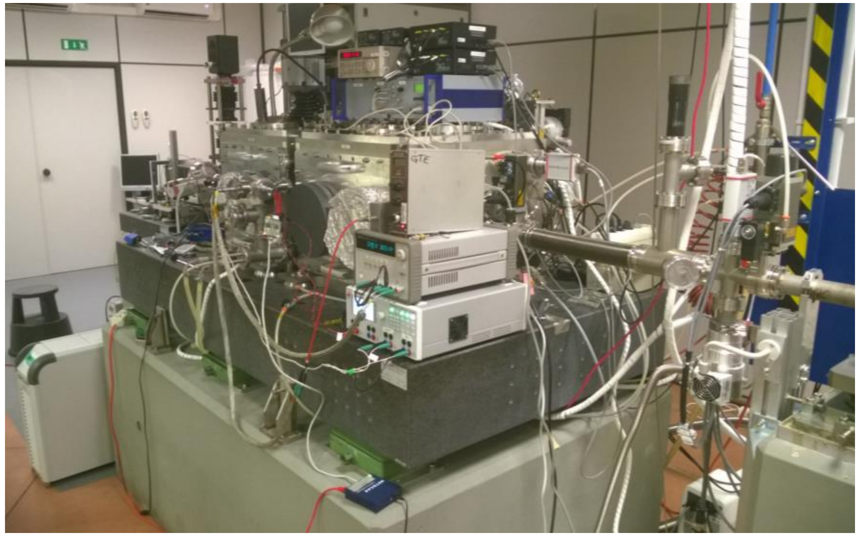

The microscope is operated in the 400 - 2200 eV photon energy range

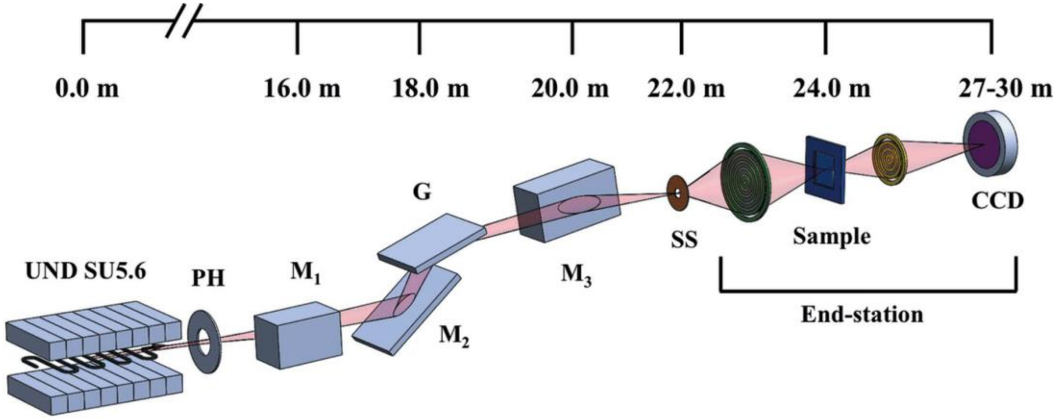

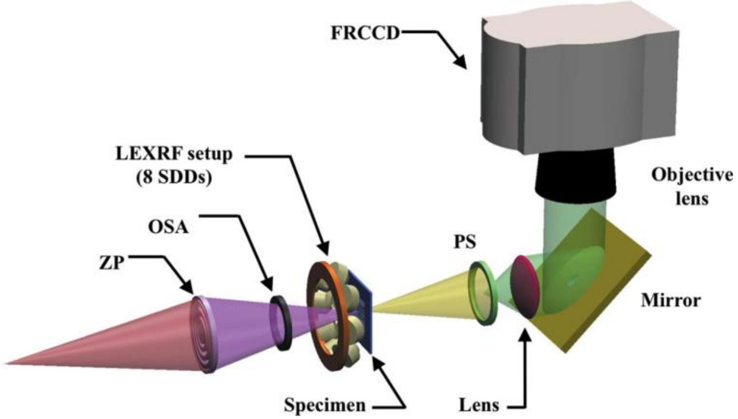

Gianoncelli A., et al. "Current status of the TwinMic beamline at Elettra: a soft X-ray transmission and emission microscopy station." *Journal of Synchrotron radiation* 23.6 (2016): 1526-1537.

Comparison: current vs new Detector Systems (TM)

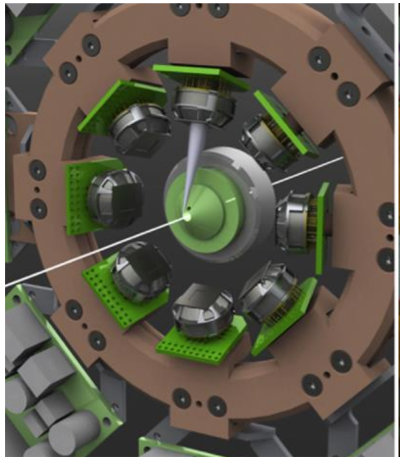
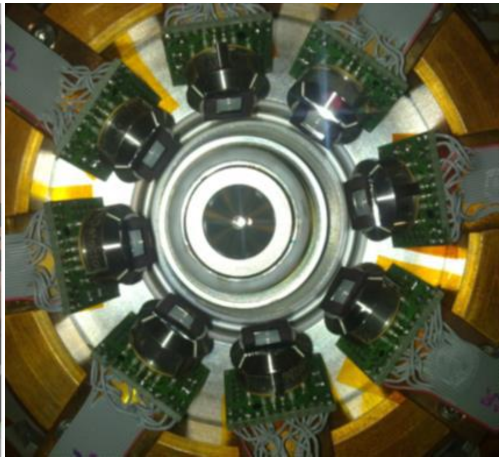
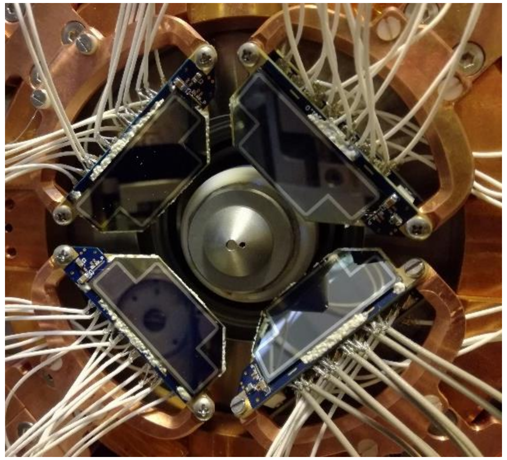
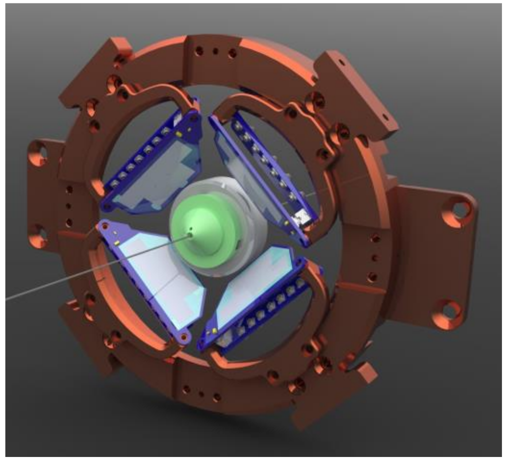

	Current TwinMic detector system	Novel SDD detector system
Detectors – Total N. of Channels	8 - 8	4 - 32
Total active area [mm^2]	240	1230
Solid angle [%]	4	27
Counts [kcounts/s]	35,1	195,0
Counts gain [%]	100	556
Experiment time equivalent [hh:mm]	10:00	1:48

Detector System TM (TwinMic of Elettra)

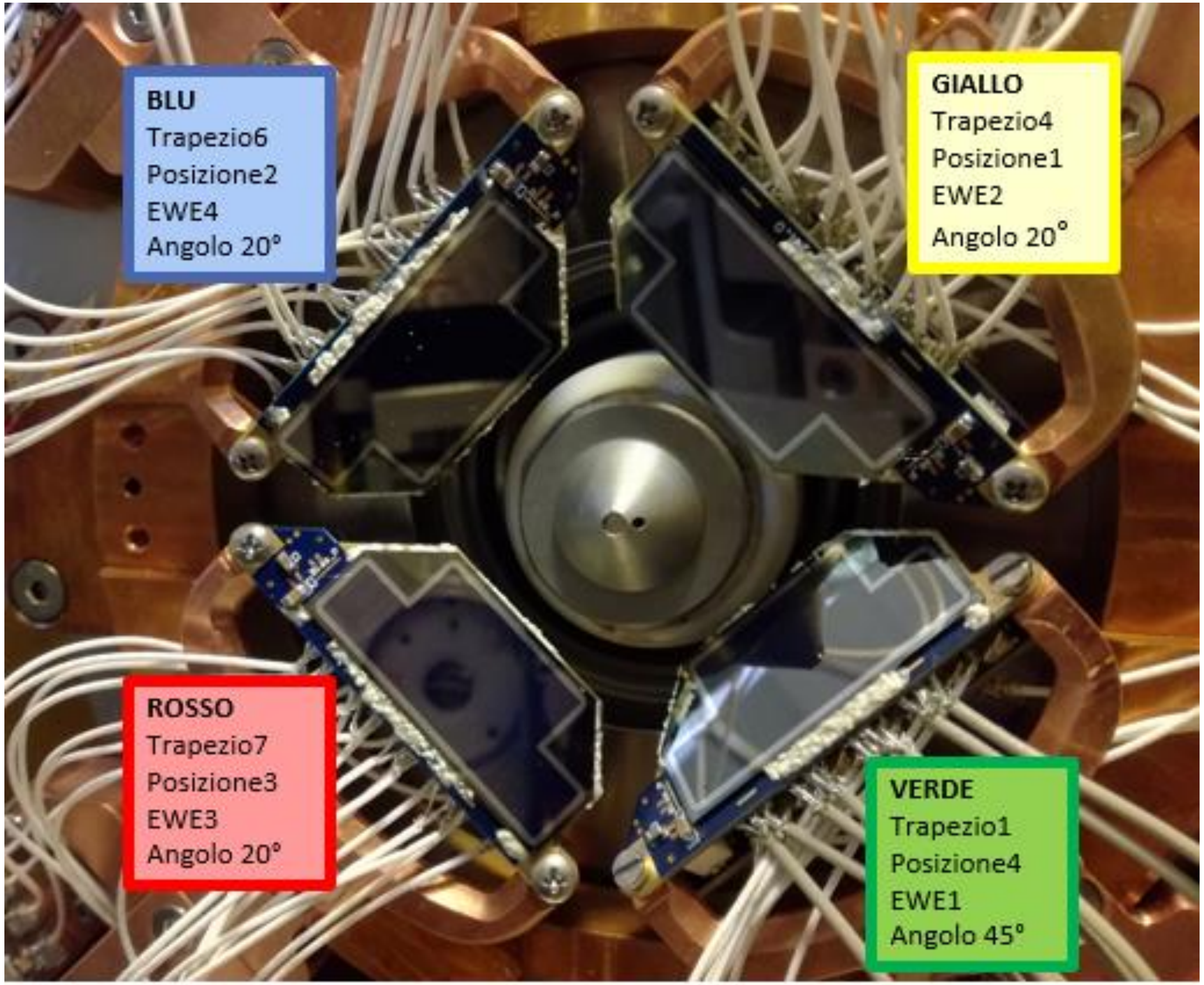

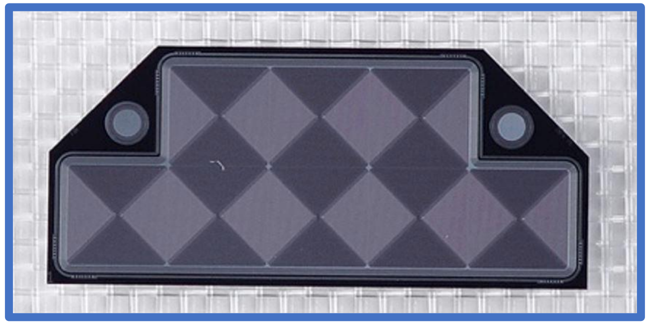

1 trapezium:
8 ch each of
6.2 x 6.2 mm^2 area

4 trapezium:
32 ch, total area: 1113 mm^2 collimated area

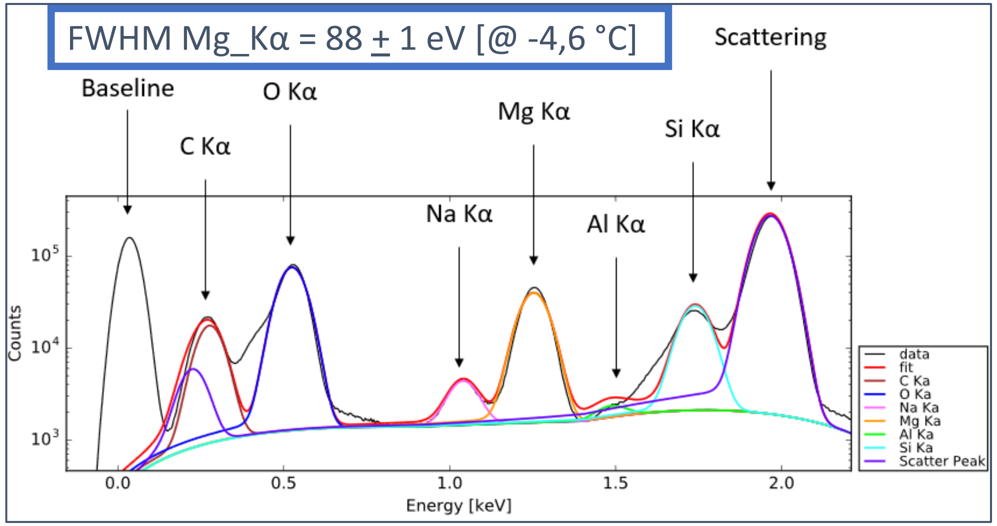

Soybean root sample -
ch4_trap1_green 30 min

DS-TM: XRF Topography with structure1

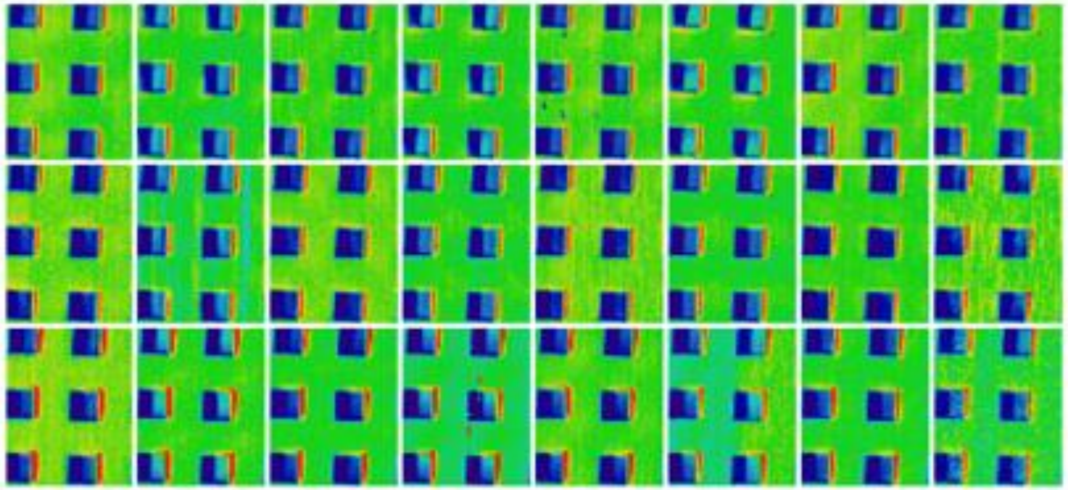

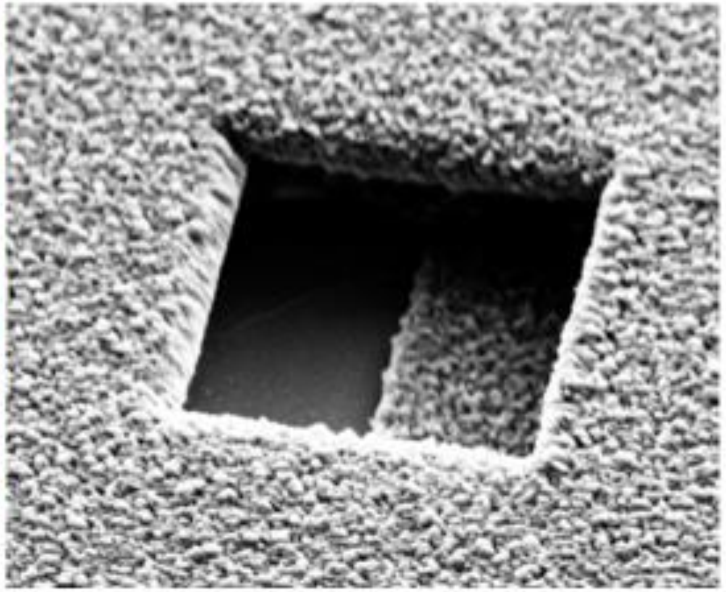

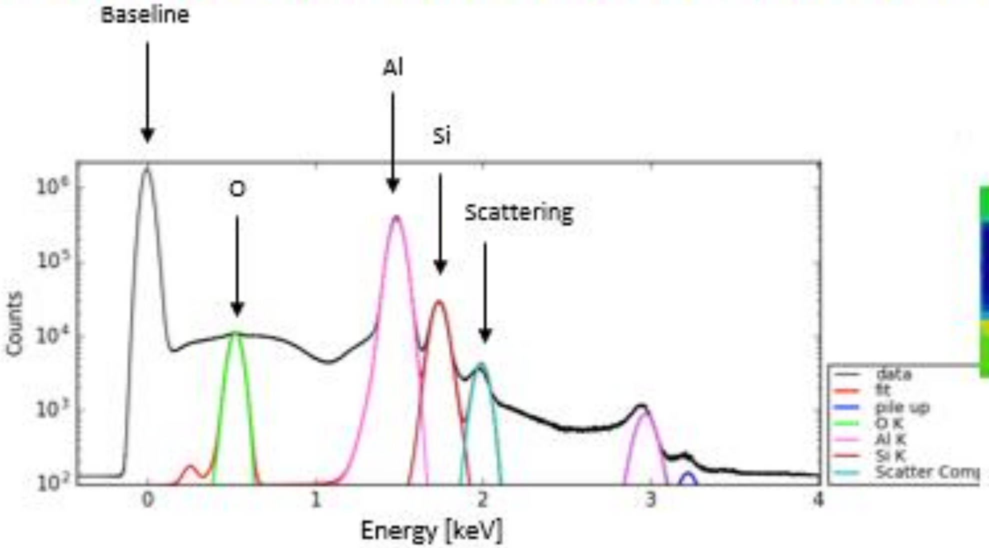

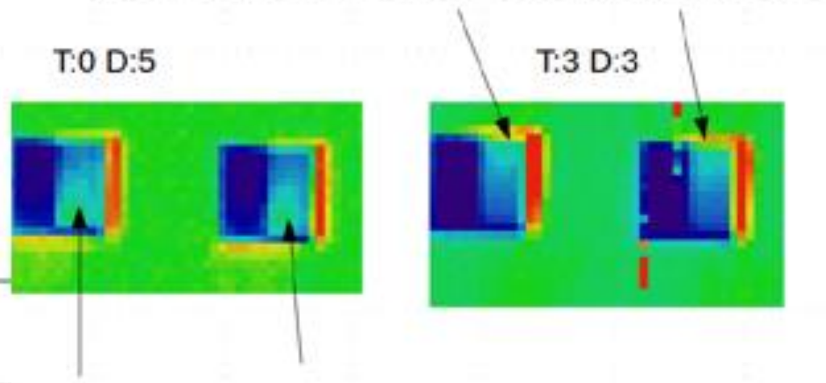

Conclusions

- SDDs have very **good performance** and are a very important **scientific and technological instrument**
- **Versatile dedicated design** of detectors system
  - Very good energetic resolution
  - Work at room temperature
  - Large area, in multipixel array
  - Low dead time
  - High count rate
- Numerous **important applications** of the detector system:
  - Agricultural and food chain (pollutants and contaminants)
  - Biophysics
  - Materials science and industry
  - Cultural heritage

References

- Cirrincione, D., et al. "A new collimated multichannel modular detection system based on Silicon Drift Detectors." Nuclear Instruments and Methods in Physics Research Section A: Accelerators, Spectrometers, Detectors and Associated Equipment 1049 (2023): 168118.
- Vacchi, A., et al. "Recent progress in high resolution X-ray customised detection systems." Journal of Physics: Conference Series. Vol. 2380. No. 1. IOP Publishing, 2022.
- Carlomagno, Ilaria, et al. "Trace-element XAFS sensitivity: a stress test for a new XRF multi-detector." Journal of Synchrotron Radiation 28.6 (2021): 1811-1819.
- Cirrincione, D. "First characterization of the detector system for the XAFS beam-line of the synchrotron light source SESAME." Il nuovo cimento C 42.5 (2019): 1-8.
- Rachevski, Alexander, et al. "The XAFS fluorescence detector system based on 64 silicon drift detectors for the SESAME synchrotron light source." Nuclear Instruments and Methods in Physics Research Section A: Accelerators, Spectrometers, Detectors and Associated Equipment 936 (2019): 719-721.
- Kourousias, G., et al. "XRF topography information: Simulations and data from a novel silicon drift detector system." Nuclear Instruments and Methods in Physics Research Section A: Accelerators, Spectrometers, Detectors and Associated Equipment 936 (2019): 80-81.
- Bufon, J., et al. "Large solid angle and high detection efficiency multi-element silicon drift detectors (SDD) for synchrotron based X-ray spectroscopy." AIP Conference Proceedings. Vol. 2054. No. 1. AIP Publishing LLC, 2019.
- Bufon, J., et al. "A new large solid angle multi-element silicon drift detector system for low energy X-ray fluorescence spectroscopy." Journal of Instrumentation 13.03 (2018): C03032.

THANKS FOR YOUR ATTENTION

Output Count Rate (OCR)

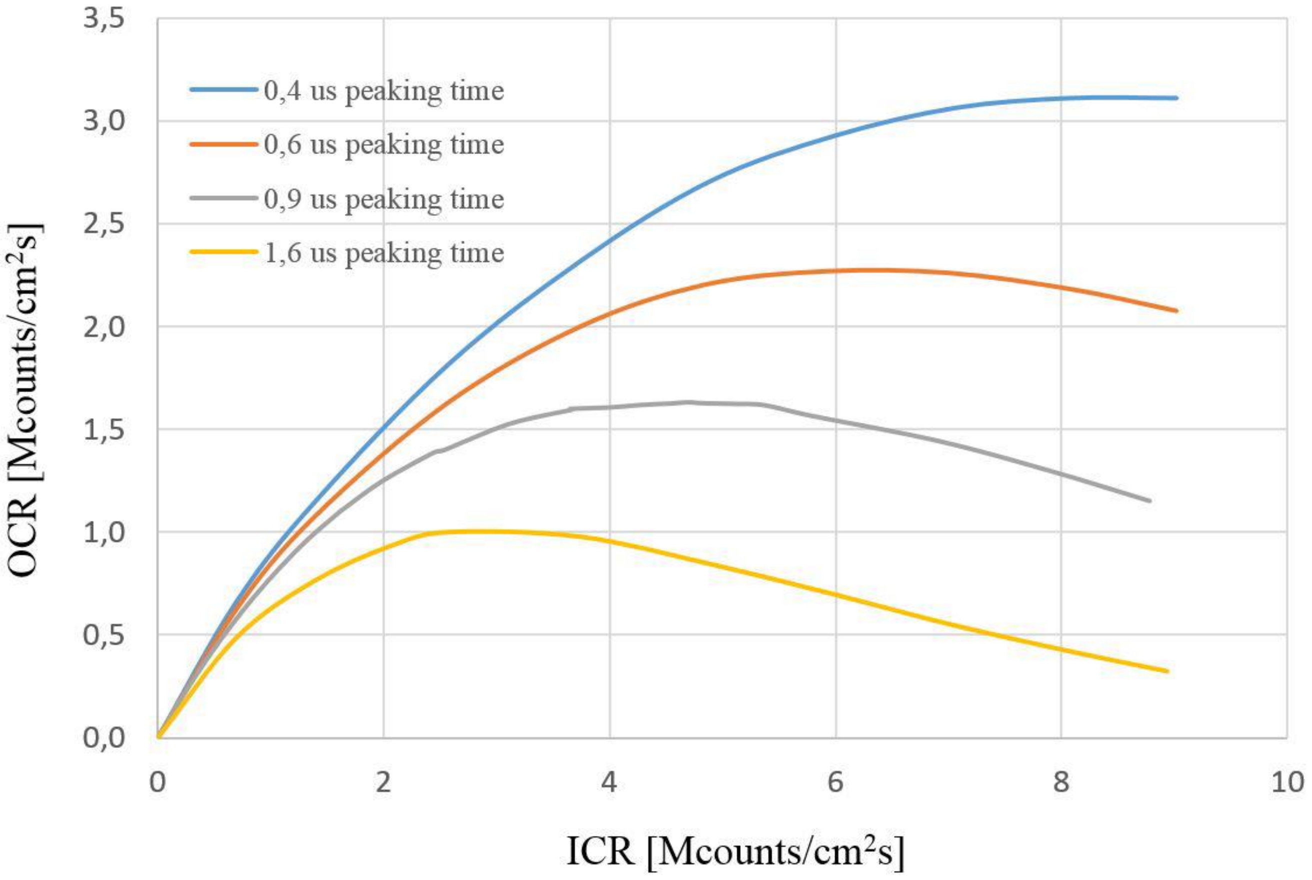

Output count-rate (OCR) versus input count-rate (ICR), obtained with different peaking time ranging from 0.4 to 1.6 µs. Test with 13 active cells to confirm the ability of the new system to work at high input count-rates (ICR) while maintaining low dead time and a good energy resolution. This translates into an output count-rate (OCR) of 15.5 Mcount/s for the entire 64 elements collimated detector.

Bufon, J., et al. "Large solid angle and high detection efficiency multi-element silicon drift detectors (SDD) for synchrotron based X-ray spectroscopy." *AIP Conference Proceedings*. Vol. 2054. No. 1. AIP Publishing LLC, 2019.